


Phase diagram of an interacting staggered Su-Schrieffer-Heeger two-chain ladder close to a quantum critical point

A. A. Nersesyan 

*The Abdus Salam International Centre for Theoretical Physics, 34151 Trieste, Italy;
Tbilisi State University, Andronikashvili Institute of Physics, 0177 Tbilisi, Georgia;
and Ilia State University, 0162 Tbilisi, Georgia*



(Received 20 May 2020; revised 22 June 2020; accepted 22 June 2020; published 6 July 2020)

We study the ground-state phase diagram of an interacting staggered Su-Schrieffer-Heeger (SSH) ladder in the vicinity of the Gaussian quantum critical point. The corresponding effective field theory, which nonperturbatively treats correlation effects in the ladder, is a double-frequency sine-Gordon (DSG) model. It involves two perturbations at the Gaussian fixed point: the deviation from criticality, and umklapp scattering processes. While massive phases with broken symmetries are identified by means of local order parameters, a topological distinction between thermodynamically equivalent phases becomes feasible only when nonlocal fermionic fields, parity, and the string order parameter are included in consideration. We prove that a noninteracting fermionic staggered SSH ladder is exactly equivalent to an $O(2)$ -symmetric model of two decoupled Kitaev-Majorana chains, or two one-dimensional p -wave superconductors. Close to the Gaussian fixed point, the SSH ladder maps to an Ashkin-Teller-like system when interactions are included. Thus, the topological order in the SSH ladder is related to broken-symmetry phases of the associated quantum spin-chain degrees of freedom. The obtained phase diagram includes a Tomonaga-Luttinger liquid state that, due to umklapp processes, can become unstable against either spontaneous dimerization or the onset of a charge-density wave (CDW). In these gapped phases, elementary bulk excitations are quantum kinks carrying the charge $Q_F = 1/2$. For sufficiently strong, long-range interactions, the phase diagram of the model exhibits a bifurcation of the Gaussian critical point into two outgoing Ising criticalities. The latter sandwich a mixed phase in which dimerization coexists with a site-diagonal CDW. In this phase, elementary bulk excitations are represented by two types of topological solitons carrying different fermionic charges, which continuously interpolate between 0 and 1. This phase has also mixed topological properties with coexisting parity and string order parameters.

DOI: [10.1103/PhysRevB.102.045108](https://doi.org/10.1103/PhysRevB.102.045108)

I. INTRODUCTION

The Su-Schrieffer-Heeger (SSH) model [1] describes a one-dimensional Peierls insulator [2] in terms of tight-binding fermions whose hopping along the chain is characterized by alternating nearest-neighbor amplitudes $t_{\pm} = t_0 \pm \Delta/2$. It was introduced four decades ago almost simultaneously with a closely related field theory of (1+1)-dimensional fermions coupled to a semiclassical scalar field with a solitonlike background—the Jackiw-Rebbi model [3]. In these seminal works it has been demonstrated that, for certain chains with a degenerate gapped ground state, such as *trans*-polyacetylene, the excitations associated with topological defects and edge states in finite samples are characterized by fractionalization of charge [3,4] and the related phenomenon of charge-spin separation [1].

Shortly after the SSH papers [1], a two-chain SSH ladder model was proposed to explain soliton confinement in arrays of weakly coupled dimerized chains [5,6]. Nowadays, low-dimensional objects such as dimerized chains and ladders are being successfully manufactured and studied in cold-atom systems on optical lattices [7–10]. Current interest in two- and multichain SSH ladders and related systems, which include hybrid models that interpolate between the

SSH and Kitaev's p -wave superconducting chain [11], as well as Creutz-Hubbard and Kitaev ladders, is strongly enhanced by the interest in the studies of topological phases of such objects [12–18]. Boundary zero-mode states characterizing such phases are believed to play an important role because of their potential for quantum computation [11,19].

The SSH ladder is described by the Hamiltonian

$$H = H_0 + H_{\text{int}},$$

where

$$H_0 = - \sum_{n\sigma} \left[t_0 + \frac{1}{2} \Delta_{\sigma} (-1)^n \right] (c_{n\sigma}^{\dagger} c_{n+1,\sigma} + \text{H.c.}) - t_{\perp} \sum_{n\sigma} c_{n\sigma}^{\dagger} c_{n,-\sigma} \quad (1)$$

is a one-particle Hamiltonian of spinless (e.g., fully-spin-polarized) noninteracting fermions, which includes dimerization (Δ_{σ}) and single-particle interchain hopping (t_{\perp}). Here, $c_{n\sigma}^{\dagger}, c_{n\sigma}$ are second-quantized operators of a fermion on the site n of the chain labeled by $\sigma = \pm 1$. The average number of fermions per single rung of the ladder is 1. The model acquires features of a strongly correlated one-dimensional (1D) Fermi system when interaction between the fermions is included. If

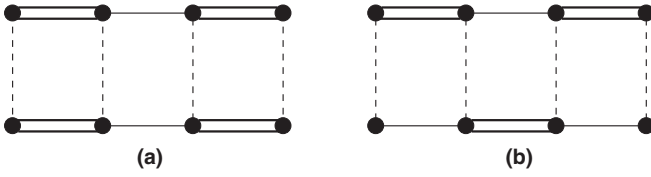


FIG. 1. Two dimerization patterns of the ladder: (a) columnar dimerization; (b) staggered dimerization. The links with hopping amplitudes t_+ , t_- , and t_\perp are depicted by the double, single, and dashed lines, respectively.

one accounts for nearest-neighbor interaction only, H_{int} takes the form

$$H_{\text{int}} = U \sum_n \hat{n}_{n,\uparrow} \hat{n}_{n,\downarrow} + V \sum_{n\sigma} \hat{n}_{n,\sigma} \hat{n}_{n+1,\sigma}, \quad (2)$$

where $\hat{n}_{n,\sigma} = c_{n\sigma}^\dagger c_{n\sigma}$ are fermionic occupation number operators, and the coupling constants U and V parametrize the interchain and in-chain repulsion. H_{int} may also incorporate longer-range interactions between the particles. Indeed, in Fermi mixtures of ultracold atoms, the properties of a lower-dimensional subsystem, such as a single chain or two-leg ladder, can be manipulated by tuning parameters in the higher-dimensional species to which the lower-dimensional subsystem is coupled. This is one way in which long-range interaction in ladder Fermi systems on optical lattices can be generated [20,21].

Figure 1 shows two paradigmatic dimerization patterns: (a) *columnar* dimerization with $\Delta_+ = \Delta_-$, and (b) *staggered* dimerization with $\Delta_+ = -\Delta_-$. In earlier theoretical [5] and experimental [22] studies it has been indicated that in quasi-1D systems of polyacetylene chains already a weak interchain tunneling makes the staggered relative ordering of the chains more stable. Apart from this, for purely theoretical reasons the *B*-type ladder appears to be of particular interest. In a columnar ladder the role of the amplitude t_\perp is similar to that of the chemical potential in a usual two-band insulator. The interchain hopping only controls the filling of the bands and thus can lead to insulator-metal (or commensurate-incommensurate [23,24]) transitions, without affecting the dispersion of the bands. At $t_\perp = 0$, the midgap states realized in the bulk as a pair of solitons centered in the vicinity of the same rung or, in the topological gapped phase, on the boundaries of the sample, are doubly degenerate zero-energy modes, each carrying fractional charge $q_F = 1/2$. These modes split into doublets due to interchain tunneling. As first shown by Baeriswyl and Maki [5], the two zero modes confine [5,6] to form a bound state representing a single fermion with the charge $q_F = 1$. Thus, at any nonzero t_\perp , degenerate boundary modes and the associated fractional charge are no longer the property of a columnar ladder.

The situation is different in the staggered SSH ladder. Here t_\perp couples to a nonconserved quantity, which makes the spectrum of the system essentially dependent on t_\perp , similar to that in the Kitaev model of a 1D *p*-wave superconductor [11]. However, there is a principal difference here: the global $U(1)$ symmetry of a staggered dimerized ladder leads to conservation of the total particle number \mathcal{N} , whereas the Kitaev

model has only a discrete symmetry \mathbb{Z}_2 , “generated” by parity $P = (-1)^{\mathcal{N}}$.

With regard to the bulk properties of the *B*-ladder, at any nonzero Δ it does not have a metallic phase occupying a finite region in the parameter space. Instead, at $t_\perp = \pm 2t_0$ already a noninteracting staggered ladder displays two symmetric Gaussian critical points separating a topologically nontrivial massive phase ($|t_\perp| < 2t_0$) from trivial phases ($|t_\perp| > 2t_0$). Due to chiral symmetry, the phase at $|t_\perp| < 2t_0$ is topologically protected and characterized by edge states with a fractional charge $q_F = 1/2$. For noninteracting fermions, the charge of elementary bulk excitations is, of course, $Q_F = 1$.

In this work, we focus on the correlation effects in an interacting staggered SSH ladder in the vicinity of the Gaussian criticality where the fermionic spectrum is gapless. Due to the $t_\perp \rightarrow -t_\perp$ symmetry, we choose t_\perp to be close to $2t_0$. We derive an effective low-energy field-theoretical model in which interaction is treated nonperturbatively using Abelian bosonization. We show that close to Gaussian criticality, interactions transform the ladder to a strongly correlated 1D system and affect the topological properties of massive phases. The phase diagram is rich and includes massive phases with explicitly or spontaneously broken discrete symmetries. Some of these phases are topologically nontrivial and some are not. Exactly at $t_\perp = 2t_0$ the phase diagram displays a line of Gaussian critical points with continuously varying exponents (Tomonaga-Luttinger liquid). If the interaction is strong enough and/or sufficiently long-ranged, umklapp processes make the Tomonaga-Luttinger critical state unstable against *spontaneous* breakdown of either link or site parity, leading to the onset of dimerization long-range order or a charge-density wave (CDW), respectively. In these gapped phases, elementary bulk excitations are not fermions but quantum kinks carrying the charge $Q_F = 1/2$.

To have a reliable tool to distinguish between topologically distinct phases of the system, one needs a *local* representation of *nonlocal* fermionic fields: parity and string order parameter. The bosonization approach supplies these nonlocal fields with a local representation. To put this correspondence on firm ground, we need to establish contact between the ladder model and hidden Ising degrees of freedom in a symmetry-preserving way. We first demonstrate that, in any range of its parameters, a noninteracting staggered SSH ladder can be *exactly* mapped onto an $O(2)$ -symmetric model of two decoupled Kitaev-Majorana (KM) chains, or equivalently two copies of an *XY* spin-1/2 chain in a transverse magnetic field, or two decoupled 1D *p*-wave superconductors (1DPS). Bearing in mind that our ladder represents a system of two SSH chains coupled by interchain tunneling ($t_\perp \neq 0$), the possibility of such factorization appears to be a remarkable property of the model. The continuous $O(2)$ symmetry shows up as the invariance of the two KM chains under rotations of the two-component Majorana vector field.

In the vicinity of the critical point, the noninteracting ladder is equivalent to a pair of identical, weakly off-critical, decoupled quantum Ising chains. The fermionic nonlocal operators (parity and string order parameter) are then identified as products of two order or disorder Ising parameters. In this way, topological order in the ladder system is related to broken-symmetry phases of the associated quantum

spin-chain degrees of freedom. Switching on interaction between the original fermions on the ladder transforms the two decoupled Ising chains to a quantum Ashkin-Teller model [25,26]. The proof of this equivalence is one of the main results of the paper.

Here a remark is in order. When the staggered SSH ladder is considered in the vicinity of the critical point $t_{\perp} = 2t_0$, the existence of the aforementioned equivalence does not come as a revelation. The theory of a massive Dirac fermion with a marginal interaction, the so-called massive Thirring model, has long been known to be equivalent to the quantum Ashkin-Teller system of two marginally coupled quantum Ising chains [27]. On the other hand, the two theories are related to the quantum sine-Gordon model [28]. Main bosonization formulas exploring this triad of equivalence have been derived, including those that concern nonlocal fermionic fields [29,30]. Obviously, the significance of the mapping of the fermionic staggered SSH ladder onto an O(2) theory of KM chains follows from the fact that all the models involved are defined on a lattice and the mapping is exact.

We show that universal low-energy properties of the model are formed due to the interplay of two relevant perturbations: the deviation from the U(1) criticality, and umklapp processes generated by interactions. Upon bosonization, such interplay is adequately described by the quantum double-frequency sine-Gordon (DSG) model [29,30]. This theory predicts the realization of a typical Ashkin-Teller scenario: at small deviations from the Gaussian criticality, the phase diagram of the model exhibits a bifurcation of the Gaussian critical point (central charge $c = 1$) into two outgoing Z_2 or Ising criticalities (each with a central charge $c = 1/2$). The two Ising critical lines sandwich a mixed phase in which dimerization coexists with a site-diagonal CDW. In this phase, due to the CDW ordering, the charge conjugation symmetry is spontaneously broken and, as a consequence, the fermionic number Q_F is not quantized in units $1/2$ (see, e.g., Ref. [31]). Elementary bulk excitations in the mixed phase are represented by two types of topological solitons carrying different fermionic charges, which continuously interpolate between 0 and 1. This phase has also mixed topological properties with continuously varying parity and string order parameters.

The paper is organized as follows. In Sec. II we overview the spectral properties of a noninteracting staggered SSH ladder. In particular, we discuss the evolution of the fermionic spectrum on approaching the critical point $t_{\perp} = 2t_0$. On decreasing the parameter $\gamma = 1 - t_{\perp}/2t_0$ ($|\gamma| \ll 1$), at small $\delta = \Delta/2t_0$, we observe a smooth crossover between an incommensurate massive phase, $\gamma > \delta^2$, and a commensurate massive phase, $\gamma < \delta^2$ (the commensurate phase extends to the region $\gamma < 0$). In the latter case, the elementary excitation represents a Dirac-like fermion with a mass $m \sim \gamma$. At $m = 0$ one has a continuum theory of a massless fermion with a single Fermi point at $k = 0$. In Sec. III we incorporate interactions between the fermions into an effective continuum model and then bosonize it. As a result, we arrive at the DSG model where the original Dirac mass term and umklapp processes are the key perturbations to the Gaussian scalar field theory. Here we also derive the bosonized form of all local physical fields.

In Sec. IV an exact equivalence between the staggered SSH ladder and a pair of Kitaev chains is established. Close to U(1) criticality ($|\gamma| \ll 1$), interactions transform this system to a quantum Ashkin-Teller model, which makes it possible to employ the previously developed formalism that derives the low-energy projections of all physical fields of the DSG model in terms of the constituent spin degrees of freedom [30]. This equivalence proves instrumental to derive bosonized expressions for nonlocal fermionic operators, parity, and string order parameter. In Sec. V we provide a local, field-theoretical representation of the parity and string order operators, together with their representation in terms of the Ising variables. In Sec. VI we discuss in much detail the ground-state phase diagram of the staggered ladder, paying attention to quantum critical lines separating massive phases, topological properties of the latter, and the fermionic numbers carried by elementary excitations. The paper has two Appendixes in which some details of Abelian bosonization and basic facts about the Kitaev-Majorana model are compiled.

II. THE SPECTRUM OF A NONINTERACTING STAGGERED SSH LADDER

We start our discussion by providing an overview of the main properties of a noninteracting staggered SSH ladder. While the columnar ladder is symmetric under the interchange P_{12} of the two chains, the Hamiltonian of the staggered ladder has a glide reflection symmetry [10] that is a direct product of a translation by one lattice spacing (\mathcal{T}_a) and reflection (P_{12}). The spectrum of the staggered ladder remains fully defined within the original Brillouin zone $|k| < \pi$.

Passing at each rung to bonding (b) and antibonding (a) states

$$a_k = \frac{1}{\sqrt{2N}} \sum_{n,\sigma} \sigma c_{n\sigma} e^{-ikn}, \quad b_k = \frac{1}{\sqrt{2N}} \sum_{n,\sigma} c_{n\sigma} e^{-ikn} \quad (3)$$

we represent the Hamiltonian (1) at $\Delta_+ = -\Delta_- \equiv \Delta$ as follows:

$$H_0 = \sum_{|k| < \pi} \psi_k^\dagger \hat{h}(k) \psi_k, \quad \psi_k = \begin{pmatrix} a_k \\ b_{k+\pi} \end{pmatrix},$$

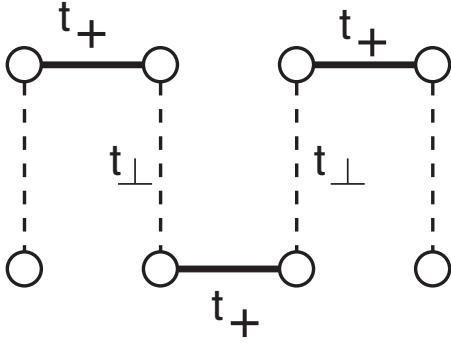
$$\hat{h}(k) = (\epsilon_k + t_{\perp}) \hat{\tau}_3 - \Delta_k \hat{\tau}_2, \quad (4)$$

where the Pauli matrices $\hat{\tau}^a$ ($a = 1, 2, 3$) act in the two-dimensional Dirac-Nambu space. Everywhere below we will assume that $t_0 > 0$, $0 < \Delta \leq 2t_0$, while the ratio $t_{\perp}/2t_0$ is arbitrary. The model (4) has a chiral symmetry, $\psi_k \rightarrow \hat{\tau}_1 \psi_k$, $\hat{\tau}_1 \hat{h}(k) \hat{\tau}_1 = -\hat{h}(k)$, implying that the spectrum of the Hamiltonian consists of $(E, -E)$ pairs,

$$E^{(\pm)}(k) = \pm E(k), \quad E(k) = \sqrt{(\epsilon_k + t_{\perp})^2 + \Delta_k^2} \quad (5)$$

and possibly contains zero-energy modes.

The Hamiltonian H_0 conserves the total charge $\mathcal{N} = \sum_k \psi_k^\dagger \psi_k$, but because of interband transitions caused by dimerization it does not conserve the “chiral charge” $\mathcal{N}_3 = \sum_k \psi_k^\dagger \hat{\tau}_3 \psi_k$. This is why, similar to the chemical potential in a BCS superconductor, t_{\perp} appears in (5) inside the square root. Therefore, there is no room for quantum commensurate-incommensurate transitions [23,24] in this case. In fact, the

FIG. 2. Staggered ladder at $t_{\perp} = t_0 - \frac{1}{2}\Delta = 0$, $t_{+} = 2t_0$.

B -ladder does not possess a metallic phase extending over a finite range of t_{\perp} . Instead at any fixed $\Delta \neq 0$ the spectrum (5) remains gapped except for two isolated critical points occurring at

$$k = 0 : \quad t_{\perp} = 2t_0 \quad (\text{upper critical point}), \quad (6)$$

$$k = \pi : \quad t_{\perp} = -2t_0 \quad (\text{lower critical point}). \quad (7)$$

These points separate massive phases that occupy the regions $|t_{\perp}| \neq 2t_0$. The criticalities belong to the universality class of a free massless fermion: Gaussian $U(1)$ criticality with central charge $c = 1$. The existence of this criticality is immediately understood in the special case

$$\Delta = 2t_0, \quad t_{+} = t_0 + \frac{\Delta}{2} = 2t_0, \quad t_{-} = t_0 - \frac{\Delta}{2} = 0 \quad (8)$$

(or equivalently $\Delta = -2t_0$, $t_{+} = 0$, $t_{-} = 2t_0$) displayed in Fig. 2. The staggered ladder transforms to a single chain with alternating hopping amplitudes $2t_0$ and t_{\perp} . Generically, the spectrum of such a chain is massive; however, at $t_{\perp} = 2t_0$ translational invariance is restored, and the resulting snake-looking uniform chain with a $1/2$ -filled tight-binding band has a gapless spectrum. A similar situation is known to exist in the theory of explicitly dimerized spin- $1/2$ Heisenberg ladders [32–34]. Notice that the conditions (6) and (7) are less restrictive than those corresponding to the translationally invariant snake-ladder of Fig. 2. In the latter case, the critical points are determined by two conditions imposed on both t_{\perp} and Δ , whereas (6) or (7) represents one condition imposed on t_{\perp} only. Therefore, on the phase plane (Δ, t_{\perp}) there exists critical *lines* $t_{\perp} = \pm 2t_0$ along which Δ may be varied.

The spectrum (5) of the noninteracting B -type SSH ladder coincides with that of a one-dimensional spinless superconductor with a p -wave pairing (1DPS)—the Kitaev model [11,19] (see Appendix B). This similarity between the staggered SSH ladder and the Kitaev model has been mentioned in the literature, and topological properties of the two models were compared [18]. In both models, the critical points $t_{\perp} = \pm 2t_0$ separate topologically nontrivial massive phases ($|t_{\perp}| < 2t_0$) from trivial massive phases ($|t_{\perp}| > 2t_0$). By the bulk-boundary correspondence [35], in both cases the topological phase shows up in the appearance of boundary zero-energy midgap states. However, there is an important difference. In the Kitaev model, the global symmetry is \mathbb{Z}_2 . Therefore, the boundary states localized at the edges of a single Kitaev chain

are Majorana zero modes [11,19]. These modes constitute a highly nonlocal realization of a \mathbb{Z}_2 -degenerate many-fermion ground state of a 1D p -wave superconductor, characterized by even and odd parity of the particle number. On the other hand, the continuous $U(1)$ symmetry of the staggered SSH ladder leads to conservation of the total particle number. Therefore, in the topologically nontrivial phase of the noninteracting staggered ladder the two degenerate boundary Majorana modes combine to produce a zero-energy state of a *complex* fermion carrying a fractional fermion number [1] $q_F = 1/2$. The situation in the interacting ladder will be discussed in Sec. VI.

The aforementioned differences make a direct mapping of the SSH ladder onto a single p -wave superconducting chain illegitimate. In Sec. IV we demonstrate that, in the absence of interaction, the staggered ladder with two SSH chains coupled by interchain tunneling is exactly equivalent to two *decoupled* Kitaev chains. Apparently, the symmetry of such a system is $\mathbb{Z}_2 \times \mathbb{Z}_2$. However, passing to a Majorana representation of the two-chain Kitaev model reveals its invariance under global $O(2)$ rotations of the two-component Majorana vector field, which correctly reproduces the $U(1)$ symmetry of the original SSH ladder model.

Let us now derive the effective fermionic Hamiltonian, which captures the low-energy properties of the noninteracting model in the vicinity of the upper critical point (6), $t_{\perp} = 2t_0$. The lower critical point (7), $t_{\perp} = -2t_0$, can be accessed using the symmetry $E(k, -t_{\perp}) = E(\pi - k, t_{\perp})$. Introducing two smooth fields slowly varying over the lattice constant a_0 ($\Lambda \lesssim 1/a_0$),

$$\begin{aligned} \psi_a(x) &= \frac{1}{\sqrt{L}} \sum_{|k| < \Lambda} e^{ikx} a_k, \\ \psi_b(x) &= \frac{1}{\sqrt{L}} \sum_{|k| < \Lambda} e^{ikx} b_{k+\pi}, \end{aligned} \quad (9)$$

we can write the Hamiltonian density as

$$\begin{aligned} \mathcal{H}^{(0)}(x) &= \Psi^\dagger(x) \left[i v_0 \partial_x \hat{\tau}_2 - \left(m + \frac{1}{2m^*} \partial_x^2 \right) \hat{\tau}_3 \right] \Psi(x) + \dots, \\ \Psi(x) &= \begin{pmatrix} \psi_a(x) \\ \psi_b(x) \end{pmatrix}. \end{aligned} \quad (10)$$

Here the dots stand for higher-order gradient terms. The parameters in (10) are

$$\begin{aligned} m &= 2t_0 - t_{\perp} \equiv 2t_0\gamma, \quad v_0 = \Delta a_0 = v_F \delta, \\ 1/2m^* &= t_0 a_0^2, \end{aligned} \quad (11)$$

$v_F = 2t_0 a_0$ being the Fermi velocity of the fermions on a single undimerized chain. Equation (10) is the Hamiltonian density of free (1+1)-dimensional fermions, which, apart from the Dirac mass m , includes a nonrelativistic correction $(m^*)^{-1} \partial_x^2$. The spectrum of $\hat{\mathcal{H}}^{(0)}$ represents a small- k expansion,

$$\begin{aligned} E^2(k) &= k^2 v_0^2 + \left(m - \frac{k^2}{2m^*} \right)^2 \\ &= m^2 + k^2 v^2 + \frac{k^4}{4m^{*2}} + \dots, \end{aligned} \quad (12)$$

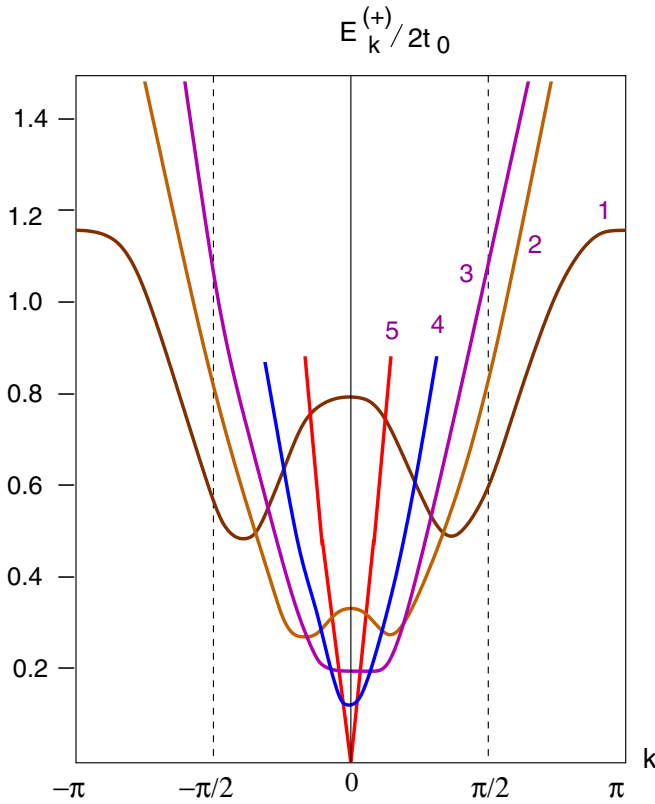


FIG. 3. The spectrum $E_k^{(+)}$ of the staggered ladder. Notations: $\tau = t_{\perp}/2t_0$, $\delta = \Delta/2t_0$. Chosen: $\delta^2 = 0.2$. Cases: (1) $\tau = 0.1$, (2) $\tau = 0.7$, (3) $\tau = 0.8$, (4) $\tau = 0.9$, and (5) $\tau = 1$.

where

$$v^2 = v_0^2 - \frac{m}{m^*} = v_F^2(\delta^2 - \gamma). \quad (13)$$

The k^4 term in (12) plays an important role in the formation of incommensurate spatial correlations of the physical quantities not too close to the critical point (the subcritical regime $\delta^2 < \gamma \ll 1$).

Let us now discuss the consequences following from the specific form of the one-particle spectrum (12) in the vicinity of the critical point, $|\gamma| \ll 1$ (see Fig. 3). We assume that $0 < \delta \ll 1$. Depending on the sign of v^2 in the expansion (12), there are two regimes within the gapped phase $0 < \gamma \ll 1$: (i) a massive *incommensurate* regime: $v^2 < 0$, $\delta^2 < \gamma \ll 1$; (ii) a massive *commensurate* regime: $v^2 > 0$, $\gamma < \delta^2 \ll 1$. In regime (i), $E(k)$ has two symmetric minima at $k = \pm k_0$, where $k_0 = a_0^{-1} \sqrt{2(\gamma - \delta^2)}$. These minima, seen in curves 1 and 2 of Fig. 3, evolve from the two original minima at the Fermi momenta $\pm k_F = \pm \pi/2a_0$ where a spectral gap opens up in the limit of two decoupled SSH chains ($t_{\perp} = 0$). On decreasing γ , the momentum k_0 decreases and vanishes at the point $\gamma = \delta^2$, where $E(k) \simeq 2t_0\gamma[1 + (ka_0)^4/8\gamma^2]$ (curve 3 in Fig. 3). Further decreasing γ makes v^2 positive, and the model crosses over to the massive region (ii) in which the dispersion curve has only one minimum at $k = 0$ (curve 4 in Fig. 3). The k^4 term in the expansion (12) can be neglected under the condition that $|k|a_0 \ll \sqrt{\delta^2 - \gamma}$. Then one arrives at the spectrum of a massive Dirac fermion $E(k) \simeq$

$\sqrt{k^2 v^2 + m^2}$. Exactly at the critical point $t_{\perp} = 2t_0$ ($\gamma = 0$) the fermion becomes massless: $E(k) = v|k|$.

If γ is negative ($t_{\perp} > 2t_0$, $m < 0$), v^2 remains positive, and the dispersion curve always has a single minimum at $k = 0$. So at small but negative γ one has the spectrum of a massive Dirac fermion.

The appearance of two spectral minima of $E(k)$ at $k = \pm k_0$ indicates that in the region (i) spatial correlations of local physical fields must exhibit incommensurate modulations with the period $2\pi/2k_0$. On the other hand, since the spectrum is gapped, these correlations should fall off exponentially at distances larger than the correlation length ξ_0 . The study of this question, which will include computation of spatial density-density correlation functions in both incommensurate and commensurate massive regimes, will be postponed until a separate publication [36]. Here we would only like to stress that, in the staggered SSH ladder, crossing the point $\gamma = \delta^2$ ($k_0 = 0$) does not have a character of a phase transition. It rather signifies a smooth crossover between the massive regimes.

III. INCLUDING INTERACTIONS

Now we turn to interaction between the fermions as described by H_{int} in Eq. (2). Naturally, correlation effects are expected to be most strongly pronounced in the vicinity of the critical points ($|t_{\perp}| \sim 2t_0$). To derive a continuum representation of H_{int} , we will ignore the k^4 -correction to the single-particle spectrum (12) and proceed from the “relativistic” model of a massive Dirac fermion, Eq. (10), with the “nonrelativistic mass” m^* sent to infinity. The SU(2) “spin” symmetry of the Hubbard on-site interaction implies that H_U is invariant under rotations in the chain space. Therefore,

$$H_U = g_U \int dx \psi_a^\dagger(x) \psi_a(x) \psi_b^\dagger(x) \psi_b(x), \quad (14)$$

where $g_U = Ua_0$ is the coupling constant. Furthermore, using the correspondence

$$c_{n\sigma}^\dagger c_{n\sigma} \rightarrow \frac{a_0}{2} [\Psi^\dagger(x) \Psi(x) + \sigma(-1)^n \Psi^\dagger(x) \hat{\tau}_1 \Psi(x)]$$

we find that

$$H_V = \frac{g_V}{2} \int dx [[\Psi^\dagger(x) \Psi(x)]^2 - [\Psi^\dagger(x) \hat{\tau}_1 \Psi(x)] \times [\Psi^\dagger(x + a_0) \hat{\tau}_1 \Psi(x + a_0)]], \quad (15)$$

where $g_V = Va_0$ is another coupling constant. It is convenient to make a chiral rotation of the spinor Ψ :

$$\Psi(x) = e^{-i\pi \hat{\tau}_1/4} \chi(x), \quad \chi(x) = \begin{pmatrix} R(x) \\ L(x) \end{pmatrix}. \quad (16)$$

Under this rotation $\hat{\tau}_2 \rightarrow -\hat{\tau}_3$, $\hat{\tau}_3 \rightarrow \hat{\tau}_2$ and the effective Dirac Hamiltonian of free massive fermions becomes

$$\mathcal{H}_0(x) = \chi^\dagger(x) [-iv_0 \partial_x \hat{\tau}_3 - m \hat{\tau}_2] \chi(x). \quad (17)$$

To find the continuum form of the interaction in the (RL) basis of single-particle states, we use the relations

$$\begin{aligned} : \psi_{a(b)}^\dagger \psi_{a(b)} : &= \frac{1}{2}(J_R + J_L) \mp \frac{i}{2}(R^\dagger L - L^\dagger R), \\ : \psi_a^\dagger \psi_a :: \psi_b^\dagger \psi_b : &= \frac{1}{4}(J_R^2 + J_L^2) + J_R J_L \\ &\quad + \frac{1}{4}[(R^\dagger L)_x (R^\dagger L)_{x+a_0} + \text{H.c.}], \end{aligned} \quad (18)$$

where $J_R =: R^\dagger R :$ and $J_L =: L^\dagger L :$ are normal ordered densities of the right and left fermions, i.e., the U(1) chiral currents (see Appendix A). Taking into account the fact that H_V maintains its structure with Ψ replaced by χ , we arrive at the following expression for the interaction density, which is parametrized by two coupling constants

$$\begin{aligned} \mathcal{H}_{\text{int}} &= \frac{1}{2}g_+(J_R^2 + J_L^2) + 2g_+ J_R J_L \\ &\quad + \frac{1}{2}g_- [(R^\dagger L)_x (R^\dagger L)_{x+a_0} + \text{H.c.}], \\ g_\pm &= (g_U \pm 2g_V)/2. \end{aligned} \quad (19)$$

The first term on the right-hand side of (19) renormalizes the group velocity of the collective excitations, the second term is a marginal forward-scattering part of the interaction, and the last term describes umklapp processes whose correct treatment in a continuum field theory of spinless fermions requires point splitting [37].

Now we apply the bosonization method to the continuum fermionic model $\mathcal{H}_{\text{eff}}(x) = \mathcal{H}_0(x) + \mathcal{H}_{\text{int}}(x)$, where \mathcal{H}_0 and \mathcal{H}_{int} are given by Eqs. (17) and (19), respectively. The details of this derivation can be found in Appendix A, where the main steps of Abelian bosonization are briefly outlined. The bosonic counterpart of $\mathcal{H}_{\text{eff}}(x)$ represents a double-frequency sine-Gordon (DSG) model [29,30]:

$$\begin{aligned} \mathcal{H}_{\text{DSG}} &= \frac{u}{2}[\pi^2(x) + [\partial_x \phi(x)]^2] + \frac{m}{\pi\alpha} \cos \sqrt{4\pi K} \phi \\ &\quad - \frac{\tilde{g}}{2(\pi\alpha)^2} \cos \sqrt{16\pi K} \phi, \end{aligned} \quad (20)$$

where

$$K = 1 - \frac{g_+}{\pi u} + O(g^2). \quad (21)$$

The first term on the right-hand side of (20) describes a conformally invariant Gaussian model with central charge $c = 1$. $\phi(x)$ and $\pi(x)$ are the massless scalar field and its conjugate momentum, respectively, u being the renormalized velocity of collective excitations. We remind the reader that the “Dirac mass” $m \simeq 2t_0\gamma$ measures the deviation from the critical point ($\gamma = 0$). The mass and umklapp terms represent two perturbations with Gaussian scaling dimensions $d_1 = K$ and $d_2 = 4K$, respectively.

At a weak short-range repulsive interaction, the Luttinger-liquid parameter K is only slightly less than 1, and the umklapp term in (20) is strongly irrelevant ($d_2 > 2$) at the Gaussian fixed point. Since the DSG model is nonintegrable [29], the exact dependence of the Luttinger-liquid parameter K on the coupling constants is not known. To remedy this

shortcoming, we can imagine that our SSH ladder model incorporates longer-range interactions, which push this parameter to smaller values[38], including $K = 1/2$. Below this value, both the mass and umklapp terms become relevant, and the interplay of the two perturbations can lead to new infrared physics.

The unrenormalized umklapp coupling constant \tilde{g} is proportional to g_- and changes its sign at $g_U = 2g_V$. Even though in the effective infrared theory the precise dependence of \tilde{g} on the bare interaction constants is not universal, there is a line in the uv plane where \tilde{g} changes its sign [39]. This fact is crucial for the physical consequences about the phase diagram of the model.

The DSG model (20) must be supplemented by the list of bosonized strongly fluctuating *local* fields.

(i) The total on-rung density fluctuation is defined as

$$\begin{aligned} : \rho(n) : &= \sum_\sigma : c_{n\sigma}^\dagger c_{n\sigma} : \rightarrow a_0 J(x), \\ J(x) &= : \Psi^\dagger(x) \Psi(x) : =: \chi^\dagger(x) \chi(x) : \\ &\rightarrow \sqrt{K/\pi} \partial_x \phi(x), \end{aligned} \quad (22)$$

and the fermion number is defined as

$$\begin{aligned} Q &= \int_{-\infty}^{\infty} dx J(x) = \sqrt{K/\pi} \Delta \phi, \\ \Delta \phi &= \phi(\infty) - \phi(-\infty). \end{aligned} \quad (23)$$

(ii) The total longitudinal and transverse bond-densities, both measured from their ground-state average values at the critical point $\gamma = 0$, are

$$\begin{aligned} : \mathcal{D}_{n,n+1} : &= (-1)^n \sum_\sigma : c_{n\sigma}^\dagger c_{n+1,\sigma} : + \text{H.c.} \\ &\rightarrow a_0 \mathcal{B}_\parallel(x), \\ : \mathcal{B}_\perp(n) : &= \sum_\sigma : c_{n\sigma}^\dagger c_{n,-\sigma} : \rightarrow a_0 \mathcal{B}_\perp(x), \\ \mathcal{B}_\parallel(x) &\sim -\mathcal{B}_\perp(x) \sim: \Psi^\dagger(x) \hat{\tau}_3 \Psi(x) := \chi^\dagger(x) \hat{\tau}_2 \chi(x) \\ &\rightarrow -(\pi\alpha)^{-1} : \cos \sqrt{4\pi K} \phi(x) :. \end{aligned} \quad (24)$$

(iii) The staggered part of the site-diagonal relative density (CDW) transforms to

$$\begin{aligned} \sigma(n) &= (-1)^n \sum_\sigma : c_{n\sigma}^\dagger c_{n\sigma} : \rightarrow a_0 \rho_{\text{CDW}}(x), \\ \rho_{\text{CDW}}(x) &= : \Psi^\dagger(x) \hat{\tau}_1 \Psi(x) := \chi^\dagger(x) \hat{\tau}_1 \chi(x) \\ &\rightarrow -(\pi\alpha)^{-1} : \sin \sqrt{4\pi K} \phi(x) :. \end{aligned} \quad (25)$$

In Sec. V we show that the above list must be complemented by two more operators, $\cos \sqrt{\pi K} \phi(x)$ and $\sin \sqrt{\pi K} \phi(x)$, which represent nonlocal fermionic fields: parity and string order parameter. The latter play a crucial role in identifying topologically nontrivial massive phases of the interacting system.

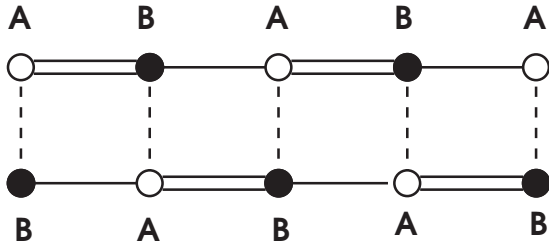


FIG. 4. Two-sublattice representation of the staggered SSH ladder.

IV. EQUIVALENCE BETWEEN THE STAGGERED SSH LADDER AND A PAIR OF KITAEV CHAINS

In this section, we establish an exact equivalence between the staggered SSH ladder and a pair of Kitaev chains. Let us divide the lattice of the staggered ladder into A and B sublattices as shown in Fig. 4. Associated with these sublattices are two fermionic operators, α_n and β_n , which are related to the original operators $c_{n\sigma}$ as follows:

$$c_{n\sigma} = (-1)^n [e^{i\pi/4} \Pi_{\sigma}(n) \alpha_n - e^{-i\pi/4} \Pi_{-\sigma}(n) \beta_n].$$

Here $\Pi_{\pm}(n) = [1 \pm (-1)^n]/2$ are projectors on the even and odd sites, respectively. We then rewrite the Hamiltonian of the noninteracting staggered SSH ladder in a translationally invariant form

$$H_0 = i \sum_n (t_+ \alpha_n^\dagger \beta_{n+1} + t_- \alpha_n^\dagger \beta_{n-1} - t_\perp \alpha_n^\dagger \beta_n) + \text{H.c.} \quad (26)$$

The spectrum of this Hamiltonian, $E^{(\pm)}(k)$, coincides with the expression (5), as it should. Splitting the operators α_n and β_n into pairs of Majorana (real) fermions (η_n^a, ζ_n^a) ,

$$\alpha_n^\dagger = \frac{\eta_n^{(1)} + i\eta_n^{(2)}}{2}, \quad \beta_n^\dagger = \frac{\zeta_n^{(1)} + i\zeta_n^{(2)}}{2},$$

$$\{\eta_n^a, \eta_m^b\} = \{\zeta_n^a, \zeta_m^b\} = 2\delta^{ab}\delta_{nm}, \quad \{\eta_n^a, \zeta_m^b\} = 0, \quad (27)$$

we find out that H_0 in (26) decouples into two identical Hamiltonians of the KM chain:

$$H_0 = \sum_{a=1,2} H_{\text{KM}}^a, \quad [H_{\text{KM}}^1, H_{\text{KM}}^2] = 0,$$

$$H_{\text{KM}}^a = \frac{i}{2} \sum_{n=1}^N (t_+ \eta_n^a \zeta_{n+1}^a + t_- \eta_n^a \zeta_{n-1}^a - t_\perp \eta_n^a \zeta_n^a). \quad (28)$$

By the correspondence discussed in Appendix B, H_0 in (28) describes two copies of the XY spin-1/2 chains in a transverse magnetic field:

$$H_0 = \sum_{a=1,2} H_{XY}^a,$$

$$H_{XY}^a = - \sum_{n=1}^N (h\sigma_{a,n}^z + J_x \sigma_{a,n}^x \sigma_{a,n+1}^x + J_y \sigma_{a,n}^y \sigma_{a,n+1}^y), \quad (29)$$

or equivalently two decoupled p -wave superconducting chains:

$$H_0 = \sum_{a=1,2} H_{\text{IDPS}}^a,$$

$$H_{\text{IDPS}}^a = \sum_n \left[-\mu_s \sum_n (f_{a,n}^\dagger f_{a,n} - 1/2) + t_s (f_{a,n}^\dagger f_{a,n+1} + \text{H.c.}) \right. \\ \left. + (\Delta_s/2) (f_{a,n}^\dagger f_{a,n+1}^\dagger + \text{H.c.}) \right], \quad (30)$$

where $f_{a,n}^\dagger = (\zeta_n^a + i\eta_n^a)/2$ ($a = 1, 2$). The parameters of the above three models are related by the formulas (B5). Notice that, according to the definition (27), the original fermionic operators α_n and β_n mix up Majorana species ($a = 1, 2$) belonging to *different* KM chains to which the Hamiltonian H_0 decouples.

According to the Jordan-Wigner equivalence (B4), the spin-fermion correspondence that relates the models (28) and (29) is highly nonlocal. Each of the two KM models ($H_{\text{KM}}^{1,2}$) or XY spin chains ($H_{XY}^{1,2}$) is \mathbb{Z}_2 -symmetric. In (28) this symmetry is realized as the invariance under transformations $\eta^a \rightarrow -\eta^a$, $\zeta^a \rightarrow -\zeta^a$, while in (29) it is the symmetry under π -rotations of the spin operators $\sigma_{a,n}^x \rightarrow -\sigma_{a,n}^x$, $\sigma_{a,n}^y \rightarrow -\sigma_{a,n}^y$. However, the sum (28) not only possesses discrete $\mathbb{Z}_2 \otimes \mathbb{Z}_2$ symmetry but it also enjoys a larger, continuous $\text{SO}(2)$ symmetry associated with global rotations of the Majorana vectors $\eta = (\eta^1, \eta^2)$ and $\zeta = (\zeta^1, \zeta^2)$. This symmetry is nonlocally realized with respect to the spin model H_0 in (29). Its existence is consistent with the $\text{U}(1)$ symmetry of the original SSH ladder model and the related conservation of the total fermion number.

Having proven an exact equivalence between a noninteracting B -type dimerized ladder and a decoupled pair of two KM copies, which holds at arbitrary nonzero t_\perp , we now specialize to the vicinity of the Ising critical point $t_\perp = 2t_0 - m$, $|m| \ll t_0$. In this limit, one can pass to a continuum description in which $\eta_n^a \rightarrow \sqrt{2a_0}\eta^a(x)$, $\zeta_n^a \rightarrow \sqrt{2a_0}\zeta^a(x)$. As a result,

$$H_{\text{KM}}^a \rightarrow \int dx \mathcal{H}_{\text{KM}}^a(x),$$

$$\mathcal{H}_{\text{KM}}^a(x) = iv\eta^a(x)\partial_x\zeta^a(x) + im\eta^a(x)\zeta^a(x) \equiv \mathcal{H}_{\text{QIC}}[\eta^a, \zeta^a], \quad (31)$$

where $v = \Delta a_0$. We see that, in the field-theoretical limit, the KM chain reduces to a model of a massive Majorana fermion, which is merely the continuum version of a slightly off-critical quantum Ising chain (QIC) [40,41]. This fact is well known: near an Ising transition, the XY spin chain in a transverse magnetic field is faithfully described by the Ising field theory [42].

A chiral rotation similar to that for the complex fermion field ψ , Eq. (16), $\xi_{R,L}^{(a)} = (\eta^a \mp \zeta^a)/\sqrt{2}$, leads to

$$H_0 \rightarrow \int dx \mathcal{H}_0(x),$$

$$\mathcal{H}_0(x) = \frac{iv}{2} (\xi_R \cdot \partial_x \xi_R - \xi_L \cdot \partial_x \xi_L) + im \xi_R \cdot \xi_L,$$

$$\xi = (\xi^{(1)}, \xi^{(2)}). \quad (32)$$

This O(2)-invariant model of a two-component massive Majorana field describes the staggered SSH ladder near the U(1) criticality in the absence of interactions. With a complex fermionic field $\chi(x)$ defined as $\chi = (\xi^{(1)} + i\xi^{(2)})/\sqrt{2}$, the model (32) is equivalent to a theory of a free massive Dirac fermion in 1+1 dimensions, given by Eq. (17).

Now we consider the structure of interaction in the KM representation. In terms of complex fermionic fields α_j and β_j , the fluctuation part of the interaction Hamiltonian (2) takes the form

$$H_{\text{int}} = \sum_j \{U\delta\rho_\alpha(j)\rho_\beta(j) + V[\delta\rho_\alpha(j)\rho_\beta(j+1) + \delta\rho_\alpha(j)\rho_\beta(j-1)]\}, \quad (33)$$

where

$$\begin{aligned} \delta\rho_\alpha(j) &= \alpha_j^\dagger \alpha_j - \frac{1}{2} = -\frac{i}{2} \eta_j^1 \eta_j^2, \\ \delta\rho_\beta(j) &= \beta_j^\dagger \beta_j - \frac{1}{2} = \frac{i}{2} \zeta_j^1 \zeta_j^2. \end{aligned}$$

So

$$H_{\text{int}} = \frac{1}{4} \sum_j \{U(\eta_{1j}\zeta_{1j})(\eta_{2j}\zeta_{2j}) + V[(\eta_{1j}\zeta_{1,j+1})(\eta_{2j}\zeta_{2,j+1}) + (\eta_{1j}\zeta_{1,j-1})(\eta_{2j}\zeta_{2,j-1})]\}. \quad (34)$$

Using the JW transformation from fermions to spin-1/2 variables (see Appendix B), it is interesting to reveal the spin-chain content of the O(2)-Majorana model with interaction (34). We find that such a fermionic model is equivalent to the following *interacting XY* spin-ladder model:

$$H_{XY}[\sigma_1, \sigma_2] = H_{XY}^1 + H_{XY}^2 + H_{XY}'[\sigma_1, \sigma_2], \quad (35)$$

where H_{XY}^a ($a = 1, 2$) are given by Eq. (29) and

$$H_{XY}'[\sigma_1, \sigma_2] = \sum_j \left[U\sigma_{1,j}^z \sigma_{2,j}^z + V \sum_{\alpha=x,y} \sigma_{1,j}^\alpha \sigma_{1,j+1}^\alpha \sigma_{2,j}^\alpha \sigma_{2,j+1}^\alpha \right] \quad (36)$$

is the interaction term. The Hamiltonian (35) can be regarded as an XY generalization of the quantum Ashkin-Teller model, the latter describing a system of two quantum Ising chains near criticality, coupled by a self-dual interaction [29,30]. This correspondence becomes relevant in the vicinity of the Gaussian transition in the original SSH ladder model. Indeed, at $t_\perp \sim 2t_0$ the interaction term (34) transforms to

$$\begin{aligned} H_{\text{int}} &= - \int dx \{U\eta_1(x)\zeta_1(x)\eta_2(x)\zeta_2(x) \\ &\quad + V[\eta_1(x)\zeta_1(x+a_0)\eta_2(x)\zeta_2(x+a_0) \\ &\quad + \eta_1(x)\zeta_1(x-a_0)\eta_2(x)\zeta_2(x-a_0)]\}. \end{aligned} \quad (37)$$

Taking the limit $a_0 \rightarrow 0$ in (37) means keeping only the part of interaction that is marginal at the ultraviolet fixed point. All neglected terms containing derivatives of the fields, including those that describe umklapp processes, are strongly irrelevant at the Gaussian fixed point of the noninteracting model. In this approximation, one arrives at the true quantum Ashkin-Teller

model

$$\begin{aligned} \mathcal{H}_{\text{AT}}(x) &= \sum_{a=1,2} i[v\eta^a(x)\partial_x \zeta^a(x) + m\eta^a(x)\zeta^a(x)] \\ &\quad + \lambda\eta^1(x)\zeta^1(x)\eta^2(x)\zeta^2(x), \end{aligned} \quad (38)$$

where $\lambda \sim g_+ \sim U + 2V$.

The model (38) is equivalent to the bosonized Hamiltonian (20) without the umklapp term. However, due to renormalizations caused by the marginal perturbation, the Luttinger-liquid parameter may reach values $K \lesssim 1/2$, in which case umklapp processes cannot be ignored. It is clear that to tackle the effects caused by the (relevant) umklapp processes would be very hard, if possible at all, in the fermionic language, Eq. (38). On the contrary, the bosonization method reformulates the emerging problem in terms of the DSG model, which allows one to infer valuable information about the phase diagram and the new emerging criticalities.

V. NONLOCAL ORDER PARAMETERS

The notion of nonlocal order in strongly correlated systems with a gapped spectrum and unbroken continuous symmetry was originally associated with the Haldane spin-liquid phase of the spin-1 chain. den Nijs and Rommelse [43] introduced a string order parameter

$$O^\alpha = \lim_{|i-j| \rightarrow \infty} \left\langle S_i^\alpha \exp \left(i\pi \sum_{k=j+1}^{i-1} S_k^\alpha \right) S_j^\alpha \right\rangle, \quad (39)$$

S_i^α ($\alpha = x, y, z$) being spin-1 operators, which takes a nonzero value in the ground state. This was shown to be related to a spontaneous breakdown of a hidden $\mathbb{Z}_2 \otimes \mathbb{Z}_2$ symmetry [44]. The Affleck-Kennedy-Lieb-Tasaki valence-bond state of a spin-1 chain [45] has revealed a deep connection between a nontrivial topological order and fourfold-degenerate spin-1/2 boundary states existing for an open chain. Later on, nonlocal string order parameters were studied in various spin chains and ladders [46] to categorize massive phases of these objects according to topologically distinct classes [47]. In recent studies, string order parameters together with another nonlocal order parameter, namely the parity operator, which arose in the context of the Kitaev 1DPS model [11,48], were extensively studied to characterize topologically trivial and nontrivial massive ground-state phases of various one-dimensional fermionic systems—SSH and Kitaev chains and their quasi-1D analogs [12,49,50].

Nonlocal string-order and parity operators relevant to our discussion were considered earlier for 1D lattice bosons [51]. Below we show that, for one-dimensional fermions, a field-theoretical representation of these nonlocal operators remains the same. Let us introduce the number of the original fermions within the interval $1 \leq j \leq n$, measured from its average value

$$\delta\mathcal{N}_n = \mathcal{N}_n - n = \sum_{j=1}^n \delta\rho_j = \sum_{j=1}^n [\delta\rho_\alpha(j) + \delta\rho_\beta(j)],$$

where $\delta\rho_j = \rho_j - 1$ is the fluctuation of the rung density. We then define the parity operator

$$\begin{aligned}\mathcal{P}_n &= e^{i\pi\delta\mathcal{N}_n} = (-1)^n \prod_{j=1}^n (1 - 2\alpha_j^\dagger \alpha_j)(1 - 2\beta_j^\dagger \beta_j) \\ &= \prod_{j=1}^n (i\eta_j^{(1)} \zeta_j^{(1)})(i\eta_j^{(2)} \zeta_j^{(2)}) = P_n^{(1)} P_n^{(2)}.\end{aligned}\quad (40)$$

The already discussed equivalence of the SSH ladder to two copies of the Kitaev chain reveals the multiplicative structure of the operator \mathcal{P}_n : it is a product of the parity operators of the two copies of the Kitaev chain to which the SSH ladder Hamiltonian maps, Eq. (28). A detailed analysis of the Majorana structure of nonlocal order parameters for an individual Kitaev model can be found in Refs. [12,52] (see also Appendix B).

According to the bosonization rules, at $n \gg 1$ the local operator $\delta\rho_n$ transforms to $(a_0/\pi)\partial_x\phi(x)$. Therefore, in the continuum limit

$$\begin{aligned}\mathcal{P}_n \rightarrow \mathcal{P}(x) &= \text{Ree} : \exp \left[i\sqrt{\pi} \int^x dy \partial_y \phi(y) \right] : \\ &= : \cos \sqrt{\pi} \phi(x) :.\end{aligned}\quad (41)$$

At the Gaussian fixed point, $\mathcal{P}(x)$ is a primary field with scaling dimension 1/4. Its nonlocal fermionic origin follows from the observation that it cannot be expressed as a linear combination of fermionic mass bilinears (the Gaussian scaling dimension of the latter is 1). At infinite separation, the two-point correlation function of local parity operators becomes

$$\lim_{|x-y| \rightarrow \infty} \langle \mathcal{P}(x) \mathcal{P}(y) \rangle = \langle P \rangle^2,$$

where $P = e^{i\pi\mathcal{N}} = P_1 P_2$ is the global parity operator, $\mathcal{N} = \mathcal{N}_N$ is the total particle number, and P_a ($a = 1, 2$) are global parities of the corresponding Kitaev chains (or related QIC models).

To obtain an equivalent representation of parity $\langle P \rangle$ in terms of the discrete (Ising) variables, one can proceed either from the factorization formula (40) and then use the results collected in Refs. [12,52], or take advantage of the correspondence between a nearly critical staggered SSH ladder and the quantum Ashkin-Teller model for which the main bosonization formulas are well known [27,30]. We will take the second route. Here one should take into account the fact that, as compared to the convention adopted in Ref. [30], in our case the sign of the Dirac (or Majorana) mass is inverted. Changing $m \rightarrow -m$ is equivalent to the duality transformation of the QIC model. With this circumstance in mind, one obtains

$$P(x) \sim \sigma_1(x) \sigma_2(x), \quad (42)$$

where $\sigma_j(x)$ ($j = 1, 2$) are local order parameters of the j th Ising copy.

We now build up a string operator:

$$O_S(n) = \exp \left(i\pi \sum_{j=1}^{n-1} \delta\rho_j \right) \delta\rho_n \equiv P_{n-1} \delta\rho_n. \quad (43)$$

In the continuum limit,

$$O_S(j) \rightarrow O_S(x) = \frac{a_0}{\pi} : \cos \sqrt{\pi} \phi(x - a_0) : \partial_x \phi(x).$$

Of interest is the string correlation function,

$$\lim_{|x-y| \rightarrow \infty} \langle O_S(x) O_S(y) \rangle = \langle O_S \rangle^2.$$

In the conformal field theory of a massless Gaussian field [53,54], Eq. (A1), the following operator product expansion can be derived:

$$\begin{aligned}\partial_x \phi(z, \bar{z}) : \cos \beta \phi(w, \bar{w}) : \\ = \frac{i\beta}{4\pi} \left(\frac{1}{z-w} - \frac{1}{\bar{z}-\bar{w}} \right) : \sin \beta \phi(w, \bar{w}) :.\end{aligned}\quad (44)$$

Here $z = v\tau + ix$, $\bar{z} = v\tau - ix$ are complex variables, τ being imaginary time. Setting $\tau = 0$ and substituting $\beta = \sqrt{\pi}$ and $z-w = \alpha$ (here α is the short-distance cutoff of the bosonic theory), up to a nonuniversal multiplicative constant, we obtain

$$O_S(x) \sim : \sin \sqrt{\pi} \phi(x) : \sim \mu_1(x) \mu_2(x), \quad (45)$$

where $\mu_{1,2}(x)$ are the Ising disorder operators of the corresponding chains. Referring for a general definition to Chap. 9 of the book by Mussardo [41] here we only mention that the existence of the disorder operator in the QIC model follows from the Kramers-Wannier duality between the ordered and disordered massive ground-state phases that map to each other under sign reversal of the Majorana mass. Physically, in the ordered Ising phase, the disorder operator $\mu(x)$ creates a kink at a point x separating \mathbb{Z}_2 -degenerate states with opposite signs of the magnetization $\langle \sigma(x) \rangle$ at $x > 0$ and $x < 0$. Kink condensation associated with the appearance of a nonzero average $\langle \mu \rangle$ leads to the onset of the disordered Ising phase.

When the marginal part of the interaction is taken into account, the compactification radius of the scalar field gets changed and $\phi(x) \rightarrow \sqrt{K} \phi(x)$. Accordingly, the parity and string operators, (41) and (45), become

$$\mathcal{P}(x) \sim : \cos \sqrt{\pi K} \phi(x) : , \quad O_S(x) \sim : \sin \sqrt{\pi K} \phi(x) : . \quad (46)$$

Thus, the nonlocal fermionic operators of the staggered SSH ladder, parity, and string order parameters admit a local representation in terms of vertex operators of the scalar field $\phi(x)$.

VI. PHASE DIAGRAM

We now turn to the low-energy effective bosonized model (20) and analyze the ground-state phase diagram of the system in the vicinity of the critical point $t_\perp = 2t_0$ ($\gamma = 0$) as a function of the Luttinger-liquid parameter K , the deviation from criticality ($m \sim \gamma$), and the umklapp coupling constant ($\tilde{g} \sim g_- \sim U - 2V$).

A. Case $1/2 < K < 2$

This is a situation when $d_1 < 2$, $d_2 > 2$, so that the umklapp term in (20) is irrelevant and the low-energy physics is described by the standard quantum sine-Gordon model,

$$\mathcal{H}(x) = \frac{u}{2} [\pi^2(x) + [\partial_x \phi(x)]^2] + \frac{m}{\pi\alpha} \cos \sqrt{4\pi K} \phi(x). \quad (47)$$

Upon renormalization, this model flows toward a strong-coupling fixed point characterized by a dynamically generated mass gap $M \sim |m|^{1/(2-K)}$. In the ground state, the field ϕ is locked in one of the degenerate minima of the cosine potential:

$$(\phi)_n = \sqrt{\frac{\pi}{K}} \left[n + \frac{1}{2} \theta(m) \right], \quad n = 0, \pm 1, \pm 2, \dots, \quad (48)$$

where $\theta(x)$ is the Heaviside step function. Since the separation of neighboring minima is $\Delta\phi = \sqrt{\pi/K}$, the fermionic number (23), associated with a topological kink of the SG model (47), is equal to $Q_F = 1$. This is the charge carried by a massive Dirac fermion. The ground state of the system is insulating.

According to (24) and (48), at any $m \neq 0$ the ground state is characterized by both the longitudinal and transverse explicit dimerization, with averages $\langle \mathcal{B}_{\parallel} \rangle$ and $\langle \mathcal{B}_{\perp} \rangle$ nonzero and of opposite sign. At the critical point, both bond densities change their sign. The system goes through a U(1) Gaussian criticality to another massive phase. At $m = 0$ the model displays the properties of a spinless Tomonaga-Luttinger liquid characterized by the absence of single-fermion quasiparticles and power-law decay of correlation functions with nonuniversal, K -dependent critical exponents (see, for a review, Refs. [38,40]).

The two massive phases with opposite signs of m are dual to each other and thermodynamically indistinguishable. However, they differ in their topological properties. The case $m < 0$ corresponds to the disordered Ising phase while $m > 0$ corresponds to the ordered phase. In a single Kitaev 1DPS chain, the Ising ordered (disordered) phases correspond to topologically nontrivial (trivial) phases of the superconductor. Then, according to the relations (42) and (45), we conclude that

$$\begin{aligned} m > 0 : \langle P \rangle &= 0, \quad \langle O_S \rangle \neq 0 \text{ (topological phase),} \\ m < 0 : \langle P \rangle &\neq 0, \quad \langle O_S \rangle = 0 \text{ (nontopological phase),} \end{aligned} \quad (49)$$

in full agreement with the different structure of the bosonic vacuum at $m > 0$ and $m < 0$ as displayed by Eqs. (48). In the phases where they are nonzero, up to a nonuniversal coefficient both parity and string order parameter scale with the bare mass m as

$$\begin{aligned} P(m) &\sim \theta(-m)F(m), \quad O_S(m) \sim \theta(m)F(m), \\ F(m) &\sim (|m|\alpha/u)^{K/4(2-K)}. \end{aligned} \quad (50)$$

On approaching the Gaussian criticality ($m \rightarrow 0$), both $P(m)$ and $O_S(m)$ vanish.

The above results for parity agree with the conclusions reached by Kitaev and co-authors [48,55], who discussed topological properties of fermions in one dimension. They argued that in the topologically trivial phase of a 1D p -wave superconductor, the ground state has a certain parity. On the other hand, in the topologically nontrivial phase with two boundary Majorana zero modes, the nonlocally realized \mathbb{Z}_2 degeneracy of the vacuum always remains unbroken, and the average parity vanishes. We see that the bosonization treatment of a pair of the Ising models to which the original SSH ladder maps supports this conclusion.

The situation with the string order parameter is just the opposite. From (49) it follows that the operator O_S acquires a

nonzero expectation value in the Ising ordered phase ($m > 0$) and vanishes in the disordered Ising phase ($m < 0$). Thus, as expected, the string order parameter is indicative of topological order in the model.

The insulating state at $m > 0$ is topologically nontrivial. For the model (47) with open boundary conditions, the spectrum contains boundary modes that transform to zero-energy midgap states in the thermodynamic limit ($L \rightarrow \infty$). It is well known [3] that each zero mode accumulates the fractional charge $q_F = 1/2$. In bosonization language this fact can be understood as follows. A boundary of a finite system, say at $x = 0$, is topologically equivalent to a mass kink of the SG model (47) which separates the topological bulk phase ($x > 0$) with $m > 0$ from the vacuum at $x < 0$, the latter treated as a phase with $m \rightarrow -\infty$. Following Jackiw and Rebbi [3], one then replaces the mass m in (47) by a coordinate-dependent function $m(x)$ with a solitonic profile: $m(x) \rightarrow m > 0$ at $x \rightarrow \infty$, $m(x) \rightarrow -\infty$ at $x \rightarrow -\infty$. The vacua corresponding to different signs of $m(x)$ have a relative shift $\Delta\phi = \sqrt{\pi/4K}$, which immediately leads to the fractional charge $q_F = 1/2$ of the zero fermionic mode at the boundary, as opposed to the unit charge of the bulk fermionic excitations. The bulk massive phase at $m < 0$ is topologically trivial: no boundary zero modes exist in this case.

It is worth noting that, in both massive phases, the link-parity symmetry (P_L) of the ground states

$$P_L : n \rightarrow 1 - n, \quad \chi(x) \rightarrow \hat{\tau}_2 \chi(-x), \quad \phi(x) \rightarrow -\phi(-x) \quad (51)$$

excludes the formation of a site-diagonal charge-density wave: $\langle \rho_{\text{CDW}} \rangle = 0$. Indeed, in the strong-coupling regime, for both sets of vacua (48) the average $\langle \sin \sqrt{4\pi K} \phi \rangle$ vanishes.

Thus the properties of the system at $1/2 < K < 2$ are controlled by the magnitude and sign of the Dirac mass m .

B. Case $K < 1/2$

A more complicated and interesting picture emerges when both perturbations in the DSG model (20) are relevant: $d_1 < d_2 < 2$. The phase diagram of the system at $K < 1/2$ is schematically depicted in Fig. 5.

Suppose that the noninteracting ladder is at the Gaussian critical point $m = 0$. When umklapp processes are taken into account, the effective low-energy theory is described by a sine-Gordon model but with a different cosine perturbation:

$$\mathcal{H}(x) = \frac{u}{2} [\pi^2(x) + [\partial_x \phi(x)]^2] - \frac{\tilde{g}}{2(2\pi\alpha)^2} \cos \sqrt{16\pi K} \phi(x). \quad (52)$$

At $K \leq 1/2$ the dynamically generated mass gap scales as $M_g \sim |\tilde{g}|^{1/(2-4K)}$. In the infrared limit, the field ϕ gets locked in one of the minima,

$$(\phi)_n = \frac{1}{2} \sqrt{\frac{\pi}{K}} \left[(n + \frac{1}{2} \theta(-\tilde{g})) \right], \quad n = 0, \pm 1, \pm 2, \dots \quad (53)$$

Since $\Delta\phi = (\phi)_{n+1} - (\phi)_n = \sqrt{\pi/4K}$, one concludes that the fermionic number carried by a quantum soliton of the SG model (52) is fractional, $Q_F = 1/2$. The critical point $\tilde{g} = 0$ separates two massive phases with different physical properties. At $\tilde{g} > 0$ $\langle \cos \sqrt{4\pi K} \phi \rangle \neq 0$, $\langle \sin \sqrt{4\pi K} \phi \rangle = 0$,

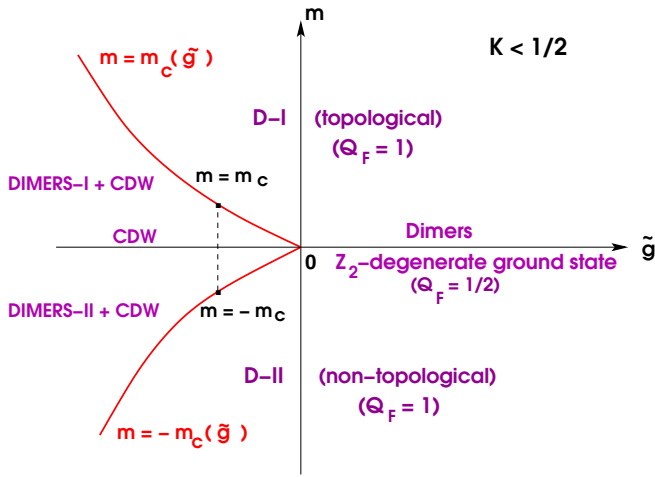


FIG. 5. Phase diagram of interacting staggered SSH ladder at $t_{\perp} \sim 2t_0$, $K < 1/2$. D-I and D-II denote nondegenerate massive phases with opposite signs of average dimerization. At $m = 0$ the ground state is twofold-degenerate and is spontaneously dimerized if $\tilde{g} > 0$ or has a site-diagonal charge-density wave if $\tilde{g} < 0$. Q_F indicates the fermionic charge of elementary excitations. $m = \pm m_c(\tilde{g})$ are critical lines belonging to the Ising universality class. A similar phase diagram for $t_{\perp} \sim -2t_0$ is obtained from the present one by a mirror reflection with respect to the horizontal axis.

so there exists a bond-density wave in the ground state of the system (dimerization). On the other hand, at $\tilde{g} < 0$ $\langle \cos \sqrt{4\pi K} \phi \rangle = 0$, $\langle \sin \sqrt{4\pi K} \phi \rangle \neq 0$, indicating the onset of a site-diagonal charge-density wave. Close to the critical point both the dimerization $\langle \mathcal{B}_{\parallel, \perp} \rangle$ and the staggered density $\langle \rho_{\text{CDW}} \rangle$ (at $\tilde{g} > 0$ and $\tilde{g} < 0$, respectively) scale as

$$|\langle \mathcal{B}_{\parallel, \perp} \rangle| \sim |\langle \rho_{\text{st}} \rangle| \sim (|\tilde{g}|/u)^{K/2(1-2K)}. \quad (54)$$

A similar phase diagram has been discussed by Haldane [37] for the XXZ spin-1/2 Heisenberg antiferromagnetic chain with competing interactions (in the latter case, by the Jordan-Wigner correspondence the Néel order translates to the CDW one).

The two massive phases have different symmetry properties. The dimerized phase is link-parity symmetric, while the site parity P_S ,

$$P_S : n \rightarrow -n, \quad \chi(x) \rightarrow \hat{\tau}_1 \chi(-x), \quad \phi(x) \rightarrow \frac{\sqrt{\pi}}{2} - \phi(-x), \quad (55)$$

is spontaneously broken. For the CDW phase the situation is just the opposite.

In both phases, the ground state is doubly degenerate. This follows from the fact that the corresponding order parameters, $\langle \cos \sqrt{4\pi K} \phi \rangle$ and $\langle \sin \sqrt{4\pi K} \phi \rangle$, have opposite signs for even and odd values of the integer n , which in (53) labels different degenerate vacua. The aforementioned quantum solitons of the SG model (52) are the kinks interpolating between the degenerate vacua. Fermions as stable quasiparticles are absent in the spectrum. In the spontaneously dimerized phase ($\tilde{g} > 0$), different degenerate vacua have different topological properties. It follows from (53) that at $\tilde{g} > 0$ the average parity and string order parameters are proportional to $\cos(\pi n/2)$ and $\sin(\pi n/2)$, respectively, implying that only one of the two

degenerate dimerized phases is topological (namely the one with n odd for which $\langle P \rangle = 0$, $\langle O_S \rangle \neq 0$) while the other is not ($\langle P \rangle \neq 0$, $\langle O_S \rangle = 0$). The CDW phase at $m = 0$, $\tilde{g} < 0$ is a “topologically mixed” phase. As seen from (53), in any of the degenerate CDW vacua both P and O_S have nonzero vacuum expectation values. We will return to this point in the sequel.

Consider now small deviations from the critical point, $m \neq 0$, keeping $K < 1/2$. Then the mass term is important, and one has to proceed from the DSG model (20) with both perturbations present. Apparently, the term $m \cos \sqrt{4\pi K} \phi$ is the most relevant perturbation. However, when m is small enough, the interplay of the two perturbations determines the nature of the infrared fixed point. The crossover to the new low-energy regime will occur when the mass gaps that would be generated separately by each of the two perturbations in Eq. (20) are of the same order:

$$(|m|\alpha/u)^{\frac{1}{2-K}} \sim (|\tilde{g}|/u)^{\frac{1}{2(1-K)}}. \quad (56)$$

If $\tilde{g} > 0$, the vacua (48) are odd and even subsets of the set (53). The m -perturbation lifts the degeneracy between the two sublattices of the potential $\tilde{g} \cos \sqrt{16\pi K} \phi$ and leads to the period doubling in ϕ -space. The new period is that of the potential $m \cos \sqrt{4\pi K} \phi$. As a result, two kinks with fractional charges $Q_F = 1/2$ confine to produce a bound state that is equivalent to recovery of the fundamental fermion with an integer charge $Q_F = 1$. Thus at $\tilde{g} > 0$ the main properties of the massive phase of the DSG model (20), including the quantum numbers of topologically stable excitations, are essentially the same as in the absence of umklapp processes. Nevertheless, as $m \rightarrow 0$, the system does go through a critical point: just due to umklapp processes the spectral mass gap $M(m)$ undergoes a discontinuity:

$$\lim_{m \rightarrow \pm 0} M(m) = \pm |M_{\tilde{g}}|.$$

The situation changes qualitatively when $\tilde{g} < 0$. Now the sets of fields (48) that minimize the potential $m \cos \sqrt{4\pi K} \phi$ do not minimize $|\tilde{g}| \cos \sqrt{16\pi K} \phi$. The DSG potential in this case undergoes a topological transition. Let us illustrate this semiclassically [29]. Consider the potential $\mathcal{U}(\varphi) = \mu \cos \varphi + g \cos 2\varphi$, where $g \sim -\tilde{g} > 0$, $\mu \sim m$, and $\varphi = \sqrt{4\pi K} \phi$. At $\mu < 4g$ the potential displays a set of degenerate minima located at

$$\varphi = \pm(\pi/2 + \eta_0), \quad \text{mod } 2\pi, \quad (57)$$

where $\sin \eta_0 = \mu/4g$. These minima are assembled in a sequence of local double-well potentials. At $\mu/4g \rightarrow \pm 1$ the two minima of each double-well potential merge ($\eta_0 \rightarrow \pi/2 \text{sgn} \mu$), and \mathcal{U} becomes 2π -periodic, with minima located either at $\varphi = (2n+1)\pi$ at $\mu > 0$ or $\varphi = 2\pi n$ at $\mu < 0$. The conditions $\mu/4g = \pm 1$ provide classical values of two symmetric critical points. The double-well potential structure of \mathcal{U} implies (in the Ginzburg-Landau sense) that the transition should belong to the Ising universality class. A quantum estimate of the Ising critical lines follows from the relation (56): up to a nonuniversal multiplicative numerical constant,

these lines are determined by the equations

$$m = \pm m_c(\tilde{g}), \quad m_c(\tilde{g}) \sim \frac{u}{\alpha} \left(\frac{|\tilde{g}|}{u} \right)^{\frac{2-K}{2(1-K)}}. \quad (58)$$

Thus, at a given $\tilde{g} < 0$, as $|m|$ is increased from $m = 0$ there exists critical values $m = \pm m_c$ at which the system undergoes a quantum Ising transition (see Fig. 5). A precise value of the phase shift η_0 in terms of the parameters m , \tilde{g} , and K is unknown. However, for us only two limiting values of η_0 are important: $\eta_0 \rightarrow 0$ at $m \rightarrow 0$ and $\eta_0 = \pm\pi/2$ at $m \rightarrow \pm m_c$. The inner region bordered by the two Ising critical lines represents a mixed phase in which dimerization $\langle B_{\parallel,\perp} \rangle \neq 0$ coexists with the site diagonal CDW, $\langle \rho_{\text{CDW}} \rangle \neq 0$ (see Fig. 5). The average dimerization $\langle B \rangle$ changes its sign at $m = 0$ but remains finite at the critical lines $m = \pm m_c$. The CDW order parameter reaches its maximum at $m = 0$, vanishes on approaching the critical lines, and remains zero in the regions $|m| > m_c$, where the P_L symmetry of the ground state is recovered.

The behavior of the system in the vicinity of each of the two Ising critical points $m = \pm m_c$ is described in terms of an effective Ising field theory. Necessary details can be found in Ref. [30]. Adopting the ultraviolet-infrared transmutation of the physical fields found in [30], we read off the singular parts of the average dimerization and CDW in the regions $|m \mp m_c| \ll m_c$:

$$\begin{aligned} \langle B_{\parallel,\perp} \rangle_m - \langle B_{\parallel,\perp} \rangle_{m_c} &\sim \pm \left(\frac{m \mp m_c}{m_c} \right) \ln \frac{m_c}{|m \mp m_c|}, \\ \langle \rho_{\text{CDW}} \rangle_m &\sim \theta(m_c - |m|) \left| \frac{m \mp m_c}{m_c} \right|^{1/8}. \end{aligned} \quad (59)$$

According to (57), in the mixed phase ($m < m_c$) the fractional soliton of the SG model (52) with $Q_F = 1/2$ splits into two topological kinks carrying charges

$$Q_F^\pm = \frac{1}{2} \mp \frac{\eta_0}{\pi}. \quad (60)$$

The existence of excitations in the mixed phase ($|m| < m_c$), carrying fermionic numbers that continuously depend on the parameter η_0 , follows from the spontaneous breakdown of charge conjugation symmetry \mathbb{C} caused by the onset of a CDW:

$$\begin{aligned} \mathbb{C} : \quad R(x) &\rightarrow R^\dagger(x), \quad L(x) \rightarrow L^\dagger(x), \quad \Phi(x) \rightarrow -\Phi(x), \\ \mathbb{C} Q \mathbb{C}^{-1} &= -Q, \quad \mathbb{C} \rho_{\text{st}} \mathbb{C}^{-1} = -\rho_{\text{st}}. \end{aligned} \quad (61)$$

The polymer *cis*-polyacetylene is an example of this kind [31]. At the Ising critical points ($\eta_0 \rightarrow \pm\pi/2$), the two kinks merge and the standard classification of integer topological quantum numbers is recovered: $Q_F = 0, 1$. It is just the singlet kink that loses its topological charge and becomes massless at $m = \pm m_c$. $Q_F = 1$ is the standard fermionic number of the explicitly dimerized phases, D-I and D-II in Fig. 5.

Some information on the topological properties of the ladder in the mixed phase of the phase diagram ($\tilde{g} < 0$, $|m| < m_c$) can be extracted from semiclassical estimates. Using the location of the minima of the DSG potential, given by (57),

for average parity and string order parameter, Eqs. (46), we obtain

$$\langle P \rangle \sim \cos(\varphi/2) = \frac{1}{\sqrt{2}} \left| \cos \frac{\eta_0}{2} - \sin \frac{\eta_0}{2} \right|, \quad (62)$$

$$\langle O_S \rangle \sim \sin(\varphi/2) = \frac{1}{\sqrt{2}} \left| \cos \frac{\eta_0}{2} + \sin \frac{\eta_0}{2} \right|. \quad (63)$$

As already mentioned, at $m = 0$ ($\eta_0 = 0$) both $\langle P \rangle$ and $\langle O_S \rangle$ are nonzero. When $m \rightarrow m_c - 0$ ($\eta_0 \rightarrow \pi/2$), $\langle P \rangle$ vanishes while $\langle O_S \rangle$ is finite. This is consistent with the fact that the phase D-I ($m > m_c$) is topologically nontrivial. On the other hand, at $m \rightarrow -m_c + 0$ ($\eta_0 \rightarrow -\pi/2$), $\langle P \rangle$ remains finite while $\langle O_S \rangle \rightarrow 0$, indicating that at the lower Ising critical point the system enters a topologically trivial phase D-II ($m < -m_c$) [56].

VII. CONCLUSION

In this paper, we have studied the ground-state phase diagram of the interacting staggered two-chain SSH ladder in the vicinity of the Gaussian critical point ($t_\perp \sim 2t_0$). We have derived a fully bosonized effective field-theoretical model to treat the correlation effects in a nonperturbative way. We have shown that such a model has the structure of the double-frequency sine-Gordon (DSG) model [29,30], Eq. (20), characterized by the existence of two perturbations at the Gaussian fixed point: the deviation from criticality parametrized in terms of a “Dirac mass” $m \sim 2t_0 - t_\perp$, $|m| \ll 2t_0$, and four-fermion umklapp scattering processes with amplitude \tilde{g} . The effects of forward scattering of the particles are phenomenologically incorporated into a Luttinger-liquid parameter K that varies in a broad interval including the region where both perturbations are relevant.

Massive phases with an explicitly or spontaneously broken symmetry have been identified by inspecting order parameters described by expectation values of local fermionic fields in the bosonic representation. The structure of the nonlocal operators, parity, and string order parameter, which identify topologically nontrivial phases, has been completely clarified as a result of a proof that a noninteracting fermionic staggered SSH ladder can be exactly mapped onto an $O(2)$ -symmetric model of two decoupled Kitaev-Majorana chains (or two 1D p -wave superconductors). In the vicinity of the Gaussian fixed point, an interacting staggered SSH ladder is equivalent to an Ashkin-Teller-like system of two coupled quantum Ising chains with a nonlocally realized $O(2)$ symmetry. This equivalence made it possible to show that topological order in the SSH ladder is related to broken-symmetry phases of the associated quantum spin-chain degrees of freedom.

At a relatively weak interaction ($1/2 < K < 2$), umklapp scattering plays a subleading role, so that the ground-state properties of the model are dominantly controlled by the magnitude and sign of the Dirac mass m . At $m = 0$, the ground state represents a Tomonaga-Luttinger liquid, but at $m \neq 0$ it is explicitly dimerized and insulating. Only the $m > 0$ massive phase, which is thermodynamically indistinguishable from its $m < 0$ counterpart, is topological. At a stronger and longer-range interaction ($K < 1/2$), both the mass and umklapp perturbations are relevant, and their interplay results in the ground-state phase diagram shown in Fig. 5. At $m = 0$ and any

nonzero \tilde{g} , the Tomonaga-Luttinger liquid becomes unstable under a transition to a spontaneously dimerized state ($\tilde{g} > 0$) or a site-diagonal CDW ($\tilde{g} < 0$). Elementary excitations are quantum solitons carrying fractional charge $Q_F = 1/2$. At $\tilde{g} > 0$ only one of the two degenerate dimerized phases is topological, whereas at $\tilde{g} < 0$ the CDW phase is a “topologically mixed” phase with the both average parity and string order parameter nonzero.

We have shown that in our model, depending on the sign of \tilde{g} , both scenarios of the DSG model are realized: kink confinement and Ising quantum transitions. At $\tilde{g} > 0$, the mass term lifts the degeneracy between the two spontaneously dimerized states and leads to confinement of two fractionally charged excitations, thus resulting in the recovery of the fundamental fermion with a unit charge $Q_F = 1$. At $\tilde{g} < 0$, the phase diagram acquires Ashkin-Teller-like features. The Gaussian critical point splits into two symmetric Ising critical lines $m = \pm m_c(\tilde{g}, K)$, $m_c(\tilde{g}, K) \sim |\tilde{g}|^{\frac{2-K}{2(1-K)}}$. These two lines sandwich a mixed massive phase in which dimerization coexists with a site-diagonal CDW. In this phase, charge conjugation symmetry is spontaneously broken and, consequently, the fermionic number Q_F is not quantized in units $1/2$. Elementary bulk excitations in the mixed phase are represented by two types of topological solitons carrying different fermionic charges, which continuously interpolate between the values $Q_F = 0$ and 1 . This phase has also mixed topological properties with continuously varying parity and string order parameters. It would be very interesting to investigate the structure and spectrum of midgap edge states in such a mixed phase.

Cold-atom setups are excellent candidates to realize a staggered dimerized ladder with a control of its main parameters. Of particular interest and importance are topological properties of this and other quasi-1D systems. There has been significant recent progress in developing novel experimental techniques using optical microscopy, aimed at observation of edge states at interfaces, separating topologically distinct phases of 1D ultracold atomic systems [8,9,15]. Remarkably, Ref. [8] reports on an experimental realization of a Dirac model with an inhomogeneous mass term, directly related to an inhomogeneous SSH chain. We hope that the methodology presented herein will soon make it possible to study topological excitations, including edge modes, in multichain SSH setups, so that the results of this paper might potentially be relevant to future experimental studies.

The approach developed in this paper for a two-chain dimerized ladder can be straightforwardly generalized to a larger number of chains. This would lead to a possibility to study correlation effects and topological properties of systems displaying quantum criticalities with non-Abelian symmetry groups. This and related questions are presently under investigation.

ACKNOWLEDGMENTS

I am grateful to Dionys Baeriswyl for bringing my attention to his earlier works on SSH ladders [5,6] and for interesting discussions. I would also like to thank Marcello Dalmonte and Pierre Fromholz for their interest in this work and helpful comments, and Rozario Fazio for his permanent support. I thank Mikheil Tsitsishvili for his cooperation in

studying the properties of the staggered SSH ladder in the massive incommensurate regime. The support from the Shota Rustaveli National Science Foundation of Georgia, SRNSF, Grant No. FR-19-11872, is gratefully acknowledged.

APPENDIX A: BOSONIZATION DICTIONARY

Here we provide some technical details related to the bosonization method [40], used in the main text. In 1+1 dimensions, free massless fermions [case $m = 0$ in Eq. (17)] are equivalent to free massless bosons:

$$\mathcal{H}_B^{(0)} = \frac{v_0}{2} [(\partial_x \Theta)^2 + (\partial_x \Phi)^2] \\ = v_0 [(\partial_x \varphi_R)^2 + (\partial_x \varphi_L)^2] = \pi v_0 (J_R^2 + J_L^2). \quad (\text{A1})$$

Here $\Phi(x) = \varphi_R(x) + \varphi_L(x)$ is a massless scalar field, $\Theta(x) = -\varphi_R(x) + \varphi_L(x)$ is the dual counterpart. The chiral currents $J_{R,L}(x)$ are expressed in terms of the chiral bosonic field $\varphi_{R,L}(x)$,

$$J_R(x) = \frac{1}{\sqrt{\pi}} \partial_x \varphi_R(x), \quad J_L(x) = \frac{1}{\sqrt{\pi}} \partial_x \varphi_L(x), \quad (\text{A2})$$

and they satisfy the U(1) Kac-Moody algebra [40]

$$[J_{R/L}(x), J_{R/L}(x')] = \pm \frac{i}{2\pi} \delta'(x - x'), \\ [J_R(x), J_L(x')] = 0. \quad (\text{A3})$$

Adding to (A1) the part of \mathcal{H}_{int} quadratic in the currents $J_{R,L}$, we define the Gaussian part of the equivalent bosonic model:

$$\mathcal{H}_{\text{Gauss}} = \frac{u}{2} \left(1 - \frac{\lambda}{2\pi u}\right) \Pi^2 + \frac{u}{2} \left(1 + \frac{\lambda}{2\pi u}\right) (\partial_x \Phi)^2, \quad (\text{A4})$$

where $u = v_0(1 + \lambda/2\pi v_0)$ is the renormalized velocity. Here $\Pi(x) = \partial_x \Theta(x)$ is the momentum conjugate to the field $\Phi(x)$. The current algebra (A3) ensures the canonical commutation relation $[\Phi(x), \Pi(x')] = i\delta(x - x')$.

The fermionic mass bilinears acquire the following bosonic representation:

$$R^\dagger L \rightarrow -\frac{i}{2\pi\alpha} e^{-i\sqrt{4\pi}\Phi}, \quad L^\dagger R \rightarrow \frac{i}{2\pi\alpha} e^{i\sqrt{4\pi}\Phi}, \quad (\text{A5})$$

where α is the ultraviolet cutoff of the bosonic theory. In particular,

$$\chi^\dagger \hat{\tau}_2 \chi = -i(R^\dagger L - \text{H.c.}) \rightarrow -\frac{1}{\pi\alpha} \cos \sqrt{4\pi}\Phi, \quad (\text{A6})$$

$$\chi^\dagger \hat{\tau}_1 \chi = R^\dagger L + \text{H.c.} \rightarrow -\frac{1}{\pi\alpha} \sin \sqrt{4\pi}\Phi. \quad (\text{A7})$$

Using point splitting, one bosonizes the umklapp operator

$$O_{\text{umkl}}(x) = (R^\dagger L)_{x,x+\alpha}^2 + (L^\dagger R)_{x,x+\alpha}^2 \\ - \frac{1}{2(\pi\alpha)^2} \cos \sqrt{16\pi}\Phi(x). \quad (\text{A8})$$

In the massless case ($m = 0$), the effective bosonic model takes the form

$$\begin{aligned}\mathcal{H}_B &= \mathcal{H}_{\text{Gauss}} + g\mathcal{O}_{\text{umkl}} \\ &= \frac{u}{2}[K\Pi^2 + K^{-1}(\partial_x\Phi)^2] \\ &\quad - \frac{g}{2(\pi\alpha)^2} \cos \sqrt{16\pi}\Phi.\end{aligned}\quad (\text{A9})$$

At a weak marginal coupling λ the parameter K is given by an expansion

$$K = 1 - \frac{\lambda}{\pi u} + O(\lambda^2) \quad (\text{A10})$$

in which only the $O(\lambda)$ -term is universal. Generally, the Luttinger-liquid parameter K decreases with increasing short-range repulsion, but for K to reach arbitrarily small values, longer-range interaction is required [38].

Rescaling the field and momentum

$$\Phi(x) = \sqrt{K}\phi(x), \quad \Pi(x) = (1/\sqrt{K})\pi(x),$$

one rewrites (A9) as

$$\begin{aligned}\mathcal{H}_B(x) &= \frac{u}{2}[\pi^2(x) + [\partial_x\phi(x)]^2] \\ &\quad - \frac{g}{2(\pi\alpha)^2} \cos \sqrt{16\pi K}\phi.\end{aligned}\quad (\text{A11})$$

Equation (A11) is a quantum sine-Gordon (SG) model that is well known to describe a 1D system of spinless fermions with a nearest-neighbor density-density interaction. Equivalently, such a model describes the scaling properties of the XXZ spin-1/2 chain [40].

At $m \neq 0$ one uses (A6) and bosonizes the Dirac mass term, in which case the effective bosonic theory transforms to the double-frequency sine-Gordon (DSG) model [29,30]:

$$\begin{aligned}\mathcal{H}_{\text{DSG}} &= \frac{u}{2}[\pi^2(x) + [\partial_x\phi(x)]^2] + \frac{m}{\pi\alpha} \cos \sqrt{4\pi K}\phi \\ &\quad - \frac{g}{2(\pi\alpha)^2} \cos \sqrt{16\pi K}\phi.\end{aligned}\quad (\text{A12})$$

APPENDIX B: KITAEV-MAJORANA CHAIN AND RELATED MODELS

In this Appendix, we collect known facts about the Kitaev-Majorana (KM) chain [11] and its equivalent representations, which are used in the bulk of this paper. The KM chain is defined on a lattice with N lattice sites in terms of a pair of Majorana lattice fields, η_n and ζ_n :

$$H_{\text{KM}}[\eta, \zeta] = i \sum_{n=1}^N (-h\eta_n\zeta_n + J_x\eta_n\zeta_{n+1} - J_y\zeta_n\eta_{n+1}). \quad (\text{B1})$$

In special cases $J_x \neq 0$, $J_y = 0$ or $J_x = 0$, $J_y \neq 0$, the Hamiltonian H_{KM} reduces to a quantum Ising chain (QIC) in the Majorana representation. In the general case $J_x \neq 0$, $J_y \neq 0$, the model (B1) constitutes a Majorana representation of the spin-1/2 XY chain in a transverse magnetic field,

$$H_{XY} = -h \sum_n \sigma_n^z - \sum_n (J_x \sigma_n^x \sigma_{n+1}^x + J_y \sigma_n^y \sigma_{n+1}^y). \quad (\text{B2})$$

The spin-chain model (B2) is in turn equivalent to the Kitaev toy model of a 1D p -wave superconductor (1DPS):

$$\begin{aligned}H_{\text{1DPS}} &= -\mu_s \sum_n \left(f_n^\dagger f_n - \frac{1}{2} \right) + t_s \sum_n (f_n^\dagger f_{n+1} + \text{H.c.}) \\ &\quad + (1/2)\Delta_s \sum_n (f_n^\dagger f_{n+1}^\dagger + \text{H.c.}).\end{aligned}\quad (\text{B3})$$

The equivalence of the three models—(B1), (B2), and (B3)—is established in two steps. First, by the Jordan-Wigner (JW) correspondence,

$$\sigma_n^z = 2f_n^\dagger f_n - 1, \quad \sigma_n^+ = 2(-1)^n f_n^\dagger e^{i\pi \sum_{j=1}^{n-1} f_j^\dagger f_j}, \quad (\text{B4})$$

H_{XY} is mapped onto H_{1DPS} . The parameters of the two models are related as

$$\mu_s = 2h, \quad t_s = J_x + J_y, \quad \Delta_s = 2(J_x - J_y). \quad (\text{B5})$$

Secondly, splitting each complex fermion into a pair of Majorana fermions [11]

$$\begin{aligned}f_n^\dagger &= (\zeta_n + i\eta_n)/2, \quad \zeta_n^\dagger = \zeta_n, \quad \eta_n^\dagger = \eta_n, \\ \{\zeta_n, \zeta_m\} &= \{\eta_n, \eta_m\} = 2\delta_{nm}, \quad \{\zeta_n, \eta_m\} = 0,\end{aligned}\quad (\text{B6})$$

one transforms H_{1DPS} to H_{KM} [η, ζ].

One can now build Majorana string operators [12,52]. Consider two-spin correlation functions for the XY spin model (B2): $\Gamma_x(1, n) = \langle \sigma_1^x \sigma_n^x \rangle$ and $\Gamma_y(1, n) = \langle \sigma_1^y \sigma_n^y \rangle$. Spin ordering in the x or y directions of spin space is determined by the asymptotic behavior of these correlation functions in the limit $n \rightarrow \infty$:

$$\lim_{n \rightarrow \infty} \Gamma_x(1, n) = \langle \sigma^x \rangle^2, \quad \lim_{n \rightarrow \infty} \Gamma_y(1, n) = \langle \sigma^y \rangle^2. \quad (\text{B7})$$

Since for any fixed spin projection ($\alpha = x, y, z$) $\sigma_1^\alpha \sigma_n^\alpha = (\sigma_1^\alpha \sigma_2^\alpha)(\sigma_2^\alpha \sigma_3^\alpha) \cdots (\sigma_{n-1}^\alpha \sigma_n^\alpha)$, from (B4) one deduces that

$$\sigma_n^x \sigma_{n+1}^x = -i\eta_n \zeta_{n+1}, \quad \sigma_n^y \sigma_{n+1}^y = i\zeta_n \eta_{n+1} \quad (\text{B8})$$

and finds out that the correlation functions $\Gamma_{x,y}(1, n)$, local in spin variables, are nonlocal in terms of the fermions, in which case they represent *string order parameters*:

$$\begin{aligned}\Gamma_x(1, n) &\equiv O_x(n) = \prod_{j=1}^{n-1} (-i\eta_j \zeta_{j+1}), \\ \Gamma_y(1, n) &\equiv O_y(n) = \prod_{j=1}^{n-1} (i\zeta_j \eta_{j+1}).\end{aligned}\quad (\text{B9})$$

In the region $|\mu_s| < 2t_s$ ($|h| < J_x + J_y$), depending on the sign of $\Delta_s = 2(J_x - J_y)$, either $\langle \sigma^x \rangle \neq 0$, $\langle \sigma^y \rangle = 0$ or $\langle \sigma^x \rangle = 0$, $\langle \sigma^y \rangle \neq 0$. Consequently, either the string order parameter $O_x(n)$ acquires a nonzero expectation value at $n \rightarrow \infty$ if $\Delta_s > 0$, or $O_y(n)$ if $\Delta_s < 0$ [52]. At $|\mu_s| > 2t_s$ ($|h| > J_x + J_y$), $\langle \sigma^x \rangle = \langle \sigma^y \rangle = 0$ and string order is absent. The direct calculations of the topological invariant [11,19] define the region $|\mu_s| < 2t_s$ where the massive phase of Kitaev's 1DPS model (B3) is topologically nontrivial. The same conclusion is reached when the string order parameters $O_{x,y}(n)$ are analyzed in the limit $n \rightarrow \infty$. This fact illustrates the efficiency of the string order in studies of the topological phases of 1D Fermi systems.

- [1] W. P. Su, J. R. Schrieffer, and A. J. Heeger, *Phys. Rev. Lett.* **42**, 1698 (1979); *Phys. Rev. B* **22**, 2099 (1980).
- [2] R. E. Peierls, *Quantum Theory of Solids* (Oxford University Press, London, 1955).
- [3] R. Jackiw and C. Rebbi, *Phys. Rev. D* **13**, 3398 (1976).
- [4] R. Jackiw and J. R. Schrieffer, *Nucl. Phys. B* **190**, 253 (1981).
- [5] D. Baeriswyl and K. Maki, *Phys. Rev. B* **28**, 2068 (1983).
- [6] D. Baeriswyl and K. Maki, *Phys. Rev. B* **38**, 8135 (1988).
- [7] X. Li, E. Zhao, and W. V. Liu, *Nat. Commun.* **4**, 1523 (2013).
- [8] M. Leder *et al.*, *Nat. Commun.* **7**, 13112 (2016).
- [9] E. J. Meier, F. A. An, and B. Gadway, *Nat. Commun.* **7**, 13986 (2016).
- [10] S.-L. Zhang and Q. Zhou, *Phys. Rev. A* **95**, 061601(R) (2017).
- [11] A. Y. Kitaev, *Phys. Usp.* **44**, 131 (2001).
- [12] Y. Bahri and A. Vishwanath, *Phys. Rev. B* **89**, 155135 (2014).
- [13] R. Wakatsuki, M. Ezawa, Y. Tanaka, and N. Nagaosa, *Phys. Rev. B* **90**, 014505 (2014).
- [14] D. Sticlet, L. Seabra, F. Pollmann, and J. Cayssol, *Phys. Rev. B* **89**, 115430 (2014).
- [15] S. Cheon, T.-H. Kim, S.-H. Lee, and H. W. Yeom, *Science* **350**, 182 (2015).
- [16] J. Jünemann, A. Piga, S.-J. Ran, M. Lewenstein, M. Rizzi, and A. Bermudez, *Phys. Rev. X* **7**, 031057 (2017).
- [17] C. Li, S. Lin, G. Zhang, and Z. Song, *Phys. Rev. B* **96**, 125418 (2017).
- [18] K. Padavic, S. S. Hegde, W. DeGottardi, and S. Vishveshwara, *Phys. Rev. B* **98**, 024205 (2018).
- [19] J. Alicea, *Rep. Prog. Phys.* **75**, 076501 (2012).
- [20] W.-M. Huang, K. Irwin, and S.-W. Tsai, *Phys. Rev. A* **87**, 031603(R) (2013).
- [21] Y. Okamoto, W.-M. Huang, K. Irwin, D. Campbell, and S.-W. Tsai, [arXiv:2004.13387](https://arxiv.org/abs/2004.13387).
- [22] C. R. Fincher, C. E. Chen, A. J. Heeger, A. G. MacDiarmid, and J. B. Hastings, *Phys. Rev. Lett.* **48**, 100 (1982).
- [23] G. I. Japaridze and A. A. Nersesyan, *Pis'ma Zh. Eksp. Teor. Fiz.* **27**, 356 (1978) [*Sov. Phys. JETP Lett.* **27**, 334 (1978)].
- [24] V. L. Pokrovsky and A. L. Talapov, *Phys. Rev. Lett.* **42**, 65 (1979).
- [25] M. Yamanaka, Y. Hatsugai, and M. Kohmoto, *Phys. Rev. B* **50**, 559 (1994).
- [26] G. Delfino and P. Grinza, *Nucl. Phys. B* **682**, 521 (2004).
- [27] J. B. Zuber and C. Itzykson, *Phys. Rev. D* **15**, 2875 (1977).
- [28] S. Coleman, *Phys. Rev. D* **11**, 2088 (1975).
- [29] G. Delfino and G. Mussardo, *Nucl. Phys. B* **516**, 675 (1998).
- [30] M. Fabrizio, A. O. Gogolin, and A. A. Nersesyan, *Nucl. Phys. B* **580**, 647 (2000); A. A. Nersesyan, in *NATO ASI/EC Summer School: New Theoretical Approaches to Strongly Correlated Systems* (Kluwer Academic, Amsterdam, 2001), p. 93120.
- [31] A. J. Niemi and G. W. Semenoff, *Phys. Rep.* **135**, 99 (1986).
- [32] M. A. Martin-Delgado, R. Shankar, and G. Sierra, *Phys. Rev. Lett.* **77**, 3443 (1996).
- [33] M. A. Martin-Delgado, J. Dukelsky, and G. Sierra, *Phys. Lett. A* **250**, 430 (1998).
- [34] Y.-J. Wang and A. A. Nersesyan, *Nucl. Phys. B* **583**, 671 (2000).
- [35] M. Z. Hasan and C. L. Kane, *Rev. Mod. Phys.* **82**, 3045 (2010).
- [36] M. Tsitsishvili and A. A. Nersesyan (unpublished).
- [37] F. D. M. Haldane, *Phys. Rev. B* **25**, 4925 (1982).
- [38] T. Giamarchi, *Quantum Physics in One Dimension* (Oxford University Press, Oxford, 2003).
- [39] E. Fradkin and J. E. Hirsch, *Phys. Rev. B* **27**, 1680 (1983).
- [40] A. O. Gogolin, A. A. Nersesyan, and A. M. Tsvelik, *Bosonization and Strongly Correlated Systems* (Cambridge University Press, Cambridge, 1998).
- [41] G. Mussardo, *Statistical Field Theory* (Oxford University Press, Oxford, 2010).
- [42] At t_{\perp} close to the other Ising critical point, $t_{\perp} = -2t_0 + m$, $|m| \ll t_0$, the KM chain maps again onto the QIC model (31) but with an inverted sign of the Majorana mass ($m \rightarrow -m$).
- [43] M. P. M. den Nijs and K. Rommelse, *Phys. Rev. B* **40**, 4709 (1989).
- [44] M. Kohmoto and H. Tasaki, *Phys. Rev. B* **46**, 3486 (1992).
- [45] I. Affleck, T. Kennedy, E. H. Lieb, and H. Tasaki, *Phys. Rev. Lett.* **59**, 799 (1987); *Commun. Math. Phys.* **115**, 477 (1988).
- [46] D. G. Shelton, A. A. Nersesyan, and A. M. Tsvelik, *Phys. Rev. B* **53**, 8521 (1996).
- [47] E. H. Kim, G. Fáth, J. Sólyom, and D. J. Scalapino, *Phys. Rev. B* **62**, 14965 (2000).
- [48] A. Kitaev and C. Laumann, Topological phases and quantum computation, in *Exact Methods in Low-dimensional Statistical Physics and Quantum Computing*, Lecture Notes of the Les Houches Summer School, Vol. 89 (Oxford University Press, Oxford, 2008), pp. 101–125.
- [49] F. Pollmann and A. M. Turner, *Phys. Rev. B* **86**, 125441 (2012).
- [50] A. Catuneanu, E. S. Sorensen, and H.-Y. Kee, *Phys. Rev. B* **99**, 195112 (2019).
- [51] E. Berg, E. G. Dalla Torre, T. Giamarchi, and E. Altman, *Phys. Rev. B* **77**, 245119 (2008).
- [52] G. Y. Chitov, *Phys. Rev. B* **97**, 085131 (2018).
- [53] P. Ginsparg, in *Les Houches Summer School in Theoretical Physics: Fields, Strings, Critical Phenomena, Session XLIX, 1988*, edited by E. Brézin and J. Zinn-Justin (Elsevier Science, Amsterdam, 1989).
- [54] P. Di Francesco, P. Mathieu, and D. Senechal, *Conformal Field Theory* (Springer, New York, 1997).
- [55] L. Fidkowski and A. Kitaev, *Phys. Rev. B* **83**, 075103 (2011).
- [56] S. Q. Shen, *Topological Insulators* (Springer, Berlin, Heidelberg, 2012).